Renewable and Sustainable Energy Reviews 208 (2025) 115015

Contents lists available at ScienceDirect

Renewable and Sustainable Energy Reviews

journal homepage: www.elsevier.com/locate/rser

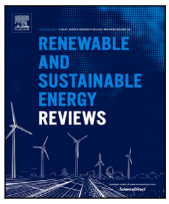

Original research article

Analysis and optimization of solid oxide fuel cell system with anode and cathode off gas recirculation

Xinyi Wei [a,b,*], Shivom Sharma [a], Jan Van herle [b], François Maréchal [a]

[a] Industrial Process and Energy Systems Engineering-École Polytechnique Fédérale de Lausanne (EPFL), Rue de l'Industrie 17, Sion, CH-1950, Valais, Switzerland
[b] Group of Energy Materials-École Polytechnique Fédérale de Lausanne (EPFL), Rue de l'Industrie 17, Sion, CH-1950, Valais, Switzerland

ARTICLE INFO

Keywords:
Solid oxide fuel cell
Anode off gas recirculation
Cathode off gas recirculation
System design
Multi-objective optimization
Heat integration

ABSTRACT

Solid oxide fuel cell technology shows great potential in generating electricity. However, insufficient steam in the stack can result in carbon deposition, accelerating cell degradation over prolonged operation. To prevent this, ensuring an adequate supply of external water is necessary, yet resulting in a larger external water purification unit and a greater need for heat for water evaporation. Anode-off gas, which comprises unreacted fuel, steam and CO_2 from the stack, can be strategically recirculated to the external reformer inlet, preventing carbon deposition in the reformer and stack. Further, solid oxide fuel cell system offers the potential to supply high-temperature heat to industrial applications, embodying the concept of combined heat and power plants. To maximize heat availability, cathode-off gas can partially be blended with the fresh air entering the stack. Various anode-off gas and cathode-off gas recirculation configurations are possible, and they have to be systematically analysed and compared. This study models all possible system configurations using different types of anode-off gas (no, cold, warm, hot) and cathode-off gas (no, warm, hot) recirculations. Multi-objective optimization has been conducted, and system performance has been analysed and compared using electrical efficiency, freshwater consumption, thermal efficiency, design complexity, heat availability and heat valorization potential. Further, an in-depth analysis of the impact of decision variables on the objective functions has been performed for different system configurations. These valuable insights serve as a guide to engineers and decision-makers, enabling informed decisions for solid oxide fuel cell system design.

1. Introduction

The escalating energy needs resulting from rapid economic and social growth have heightened the exploration and utilization of novel energy sources, including solar, wind, and hydro [1]. In recent years, there has been a noticeable increase in the examination and evaluation of these emerging energy options. Nevertheless, the incorporation of these emerging energy sources into the worldwide energy framework requires a systematic approach, given the ongoing dominance of conventional fossil fuels. Coal, oil, and natural gas jointly account for 26.9%, 33.4%, and 24.9% of the worldwide energy consumption, respectively. The widespread and dominant use of fossil fuels has a substantial impact, primarily through the release of greenhouse gases, which play a crucial role in driving global climate change. This worry is further emphasized by the substantial forecasted increase in energy-related greenhouse gas emissions; the Stated Policies Scenario (STEP) predicts that energy-related and industrial CO_2 emissions will rise to 36 gigatons annually by the year 2030 [2]. Hence, in pursuit of sustainable advancement within the energy domain, the industry should actively explore alternative technologies capable of curtailing CO_2 emissions.

Solid oxide fuel cell (SOFC) is an electrochemical device that converts fuel into electricity, achieving remarkably high electrical efficiency, above 70% [3]. This noteworthy accomplishment underscores the substantial potential of SOFC to facilitate efficient electricity generation. SOFC can be distinguished by its high-temperature operation (up to 850 °C) and high single-pass fuel utilization (up to 0.85) [4], enabling effective recuperation of heat from the exhaust gases. This attribute lends itself to advantageous applications in combined heat and power (CHP) scenarios, further enhancing the system's overall efficiency [5]. SOFC possess a remarkable characteristic of versatility when it comes to the utilization of various fuels. These fuels include hydrocarbons (gas or liquid), hydrogen, biomass and syngas. As a result, SOFC may effectively be employed in a wide range of energy applications [6]. The prospect of obtaining syngas from biomass feedstock

* Corresponding author at: Industrial Process and Energy Systems Engineering-École Polytechnique Fédérale de Lausanne (EPFL), Rue de l'Industrie 17, Sion, CH-1950, Valais, Switzerland.
E-mail address: xinyi.wei@epfl.ch (X. Wei).

https://doi.org/10.1016/j.rser.2024.115015
Received 26 September 2023; Received in revised form 17 June 2024; Accepted 16 October 2024
Available online 8 November 2024

Abbreviations

AHD	Air heater duty
AOG	Anode off gas
CA	Cold anode off-gas
CHP	Combined heat and power
COG	Cathode off gas
DV	Decision variable
EE	Electrical efficiency
ERR	External reforming ratio
ERT	External reforming temperature
EWF	External water flow
FI	Fuel input
FU	Fuel utilization
GCC	Grand composite curve
GT	Gas turbine
HA	Hot anode off-gas
HC	Hot cathode off-gas
HEX	Heat exchangers
LHV	Lower heating value
MILP	Mixed integer linear programming
MOO	Multi-objective optimization
NA	No anode off-gas
NC	No cathode off-gas
S/C	Steam-to-carbon
SOFC	Solid oxide fuel cell
RC	Rankine cycle
RR	Recirculation ratio
WA	Warm anode off-gas
WC	Warm cathode off-gas

that is sustainably maintained has the ability to meet the carbon-neutral target. Hence, SOFC technology can tackle the pressing need for greener and more sustainable power production alternatives and has the potential for decentralized power production. The presence of these influential aspects has prompted both academia and industry to dedicate significant resources to the advancement of this technology with the aim of achieving a more efficient and environmentally friendly energy system.

Although SOFC technology holds great promises, it confronts a range of challenges that warrant thoughtful consideration. A pivotal concern revolves around maintaining the requisite steam-to-carbon (S/C) ratio to avert carbon deposition — a critical necessity aligned with the minimum criteria for a stack. Traditionally, steam generation involves water evaporation; however, this engenders a need for water purification through dedicated units, escalating system cost and compounding system intricacies in terms of control. A prospective avenue for tackling this quandary involves delving into anode-off gas (AOG) recirculation. The product stream from the anodic side of the fuel cell is called AOG. Comprising modest quantities of carbon monoxide, hydrogen, and methane, predominantly carbon dioxide and water vapour, the recirculated AOG effectually facilitates internal steam recycling. This circumvents the need for steam production from water and obviates the imperative for water purification. In a broader context, this arrangement has the potential to curtail or even eliminate external water requirements.

Notably, the cathode air flow rate significantly exceeds the anode flow rate. The cathode air flow requires air heating to reach the stack inlet temperature. Two approaches are typically employed to supply this heat to the inlet air. The first approach involves employing an air-to-air heat exchanger, where outlet air from the cathodic side of SOFC exchanges heat with the inlet air. The second approach entails blending outlet streams from the stack (*i.e.*, air and unconverted fuel) within a burner, and subsequently, the downstream of the burner can engage in heat exchange with the inlet air. Irrespective of the chosen approach, a substantial portion of internal heat consumption is required by the inlet air. To address this issue, cathode off gas (COG, *i.e.*, outlet air from SOFC cathode) recirculation emerges as a viable solution. A part of the COG can be recirculated and blended with the partially heated fresh air before entering the stack. This innovation serves to diminish fresh air consumption and reduces the duty of the air heater. In turn, this reduces the size of the air heater — an essential consideration with implications for system dimensions and cost.

The research landscape on AOG and COG for SOFC systems primarily focuses on their individual impacts, with limited attention given to their combined influence. While pursuing high system efficiency remains a priority, a notable gap exists in understanding the broader implications of AOG and COG recirculations. Specifically, the importance of heat availability, thermal performance, and the integration of external water sources is often overlooked. This study systematically analyses the impact of AOG and COG modules under different operating conditions, offering valuable insights into enhancing SOFC system performance beyond mere efficiency considerations.

2. Literature review and scope of the study

2.1. Anode Off Gas (AOG) recirculation

The concept of AOG recirculation has gained significant attention in the design of SOFC systems, as it presents a promising opportunity to improve their overall performance. AOG recirculation can be achieved through a variety of approaches, including the utilization of either a low-temperature blower, a high-temperature blower, or an ejector. In the commercial market, the prevailing choice is a low-temperature blower. The AOG recirculation can be divided into three types: warm, cold, and hot. In warm AOG recirculation, the flow is cooled down before the use of a low-temperature blower. In cold AOG recirculation, the flow is cooled down, water is partially condensed, and the remaining flow is compressed by a low-temperature blower. Finally, in hot AOG recirculation, a high-temperature blower or ejector is used to increase the pressure of AOG flow. After an increase in pressure, the AOG flow is recycled back to the upstream of the pre-reformer.

The outcomes of AOG recirculation can be evaluated for scenarios characterized by high and low stack (*i.e.*, single pass) fuel utilization. In cases of high stack fuel utilization, the performance characteristics of SOFC systems exhibit a contrasting trend, as highlighted in the published research study [7]. Notably, only marginal enhancements in system (*i.e.*, global) fuel utilization are attainable through AOG recirculation. This is primarily due to the fact that a substantial portion of the available fuel is already converted within the stack. Consequently, in such circumstances, the employment of AOG recirculation can lead to disadvantages. When aiming for maximum electrical efficiency with elevated stack fuel utilization, the optimal outcome is a low recirculation rate. In cases where the stack fuel utilization rate is below 80%, an evident improvement in electrical efficiency becomes discernible with an increase in AOG recirculation. There is a corresponding rise in the system fuel utilization with an increase in AOG recirculation.

The utilization of internally generated steam offers the advantage of obviating the need for a waste heat recovery steam generator. This streamlined approach contributes to a reduction in the overall capital cost of the system. Simultaneously, this internal steam recirculation leads to a decrease in the steam content in the exhaust gas [8]. When the fuel flow rate is maintained at a lower level, and the AOG recirculation ratio is elevated, a notable decline in fuel concentration adversely affects fuel cell performance [9]. Powell et al. [10] conducted a comprehensive investigation into the interplay among global fuel utilization, AOG recirculation rate, and the lower heating value (LHV) efficiency, employing a low-temperature blower. They discerned that the influence of the AOG recirculation rate on efficiency holds greater significance due to the interplay between a reduction in the fuel concentration and

an increase in the power demand for AOG blower. Peter et al. [11] conducted an extensive examination of distinct system configurations involving SOFC systems with and without AOG recirculation, as well as the presence or absence of water condensation in the AOG line. Their findings indicated that SOFC systems without AOG recycling exhibit a notable reduction of up to 16% in electrical efficiency when contrasted with SOFC systems with AOG recycling, contingent upon operational parameters.

The primary challenges associated with high-temperature blowers lie in their relatively low efficiency and limited market availability. AVL Company has successfully engineered a high-temperature blower capable of operating at a maximum 600 °C while demonstrating an efficiency of 50% [12]. Notably, Versa Power Systems and FuelCell Energy have also developed high-temperature blowers designed to manage operating temperatures of up to 700 °C [11]. They have integrated this blower technology into the SOFC system, achieving a net DC efficiency of 64%. These developments underscore the pivotal hurdles that need to be addressed to realize the full potential of hot recirculation using blowers. Certainly, the implementation of AOG recirculation is not limited solely to the use of blowers, and it can also be achieved by employing an ejector. A noteworthy advantage of using ejectors is their exceptional high-temperature resistance, enabling high-temperature operation up to 900 °C [13]. Various research groups have delved into the design and integration of ejectors within SOFC systems. However, several challenges remain that require attention. Notably, ejectors are relatively difficult to control, particularly during part-load operations [11]. Ejector operational modes are intricately linked to system pressure, making control and sensitivity issues a noteworthy concern [14]. Another particularly critical challenge pertains to commercial viability [15]. Ejectors may not yield significant advantages within the framework of SOFC modularity, thereby impacting their feasibility for widespread commercial adoption.

SOFC system efficiency is influenced by a range of factors, including energy consumption by the air blower, losses during current collection, and the conversion from direct current to alternating current. The AOG recirculation can also contribute to a reduction in system efficiency. Of particular significance is the observation that exceeding a recirculation rate of 85% triggers a decline in efficiency, regardless of stack (*i.e.*, single pass) fuel utilization. This outcome is predominantly attributed to three pivotal factors. Firstly, recirculation blower power demand undergoes an exponential increase with AOG flow, owing to a simultaneous increase in AOG flow and anode-side pressure losses. Secondly, a recirculation rate exceeding 85% leads to disproportionate mass flow amplification. For instance, the transition from an 85% to a 90% recirculation rate results in more than a twofold surge in the power demand of the recirculation blower [16]. Thirdly, it can also be attributed to the fact that an elevated recirculation rate results in a larger portion of the AOG being composed of CO_2 and water, at the expense of H_2, CO, and CH_4. This can exert a detrimental impact on the cell voltage due to the enrichment of CO_2, which does not participate in the electrochemical reaction. Consequently, this decreases Nernst's potential within the cell. Furthermore, the heightened concentration of CO_2 has been observed to reduce catalytic activity [17].

The interplay between electrical and thermal efficiencies is predominantly influenced by two pivotal factors: fuel utilization and AOG recirculation ratio [11]. Notably, as electrical efficiency demonstrates an increase, there is typically a corresponding decrease in thermal efficiency. Thermal efficiency closely hinges on the heat generated by the combustion of unreacted fuel. As the AOG recirculation ratio is raised, a noticeable upsurge in electrical efficiency is observed. This enhancement in electrical efficiency is counterbalanced by a reduction in the available energy within the catalytic combustor. Consequently, a modest decrease in the overall efficiency becomes evident as the AOG recirculation ratio is further elevated [18]. This phenomenon is primarily attributed to the altered distribution of chemical energy within the fuel, favouring electricity generation over the conversion into heat that is removed by air cooling. Additionally, the lower sensible enthalpy or heat of the fuel compared to air also contributes to this effect [19,20]. Efficient utilization of waste heat generated by the SOFC system presents an opportunity for electricity generation [21,22].

While numerous studies have explored the impact of AOG recirculation, only a handful have examined all types of AOG recirculations, namely no AOG, cold AOG, warm AOG, and hot AOG. Furthermore, the majority of the studies have primarily focused on the electrical efficiency implications of AOG recirculation, neglecting other critical aspects. Particularly in high-temperature SOFC systems, the ability to produce heat as a co-product or to reduce the dependence on external purified water holds significant importance. These objectives are tightly interconnected with the types of AOG recirculation, yet they are often overlooked in AOG recirculation studies. Thus, considering these factors is essential for obtaining a comprehensive understanding of the broader implications of AOG recirculation in SOFC systems.

2.2. Cathode Off Gas (COG) recirculation

COG recirculation offers great potential to boost SOFC system efficiency. An air preheater requires a significant amount of heat. To tackle this issue, a strategic solution involving COG recirculation can be considered. The heat duty required by the air preheater is reduced by blending the recycled air with fresh air. A peak system efficiency has been demonstrated by combining AOG and COG recirculation with internal reforming of methane [23]. The COG recirculation can be divided into two types: warm and hot. In warm COG, the flow is cooled down before the use of a low-temperature blower, whereas, in hot COG, a high-temperature blower or ejector is used to increase the pressure of COG flow.

In the SOFC system, air on the cathodic side serves two primary purposes. Firstly, it supplies O_2^- necessary for the electrochemical conversion process, enabling the conversion of chemical energy into electricity. Secondly, it functions as a cooling medium, maintaining the required temperature difference across the stack. For the same stack power output, the use of COG recirculation requires a higher fuel flow rate [24]. It is also possible to get a high system efficiency with lower COG recirculation [25]. This is because COG recirculation lowers the oxygen partial pressure on the cathode side, which affects the efficiency of the SOFC single-pass. The COG blower may consume about 5% of the power produced by the stack. Saebea et al. [26] thoroughly assessed the performance of a SOFC-gas turbine (SOFC-GT) hybrid system by varying the COG recirculation ratio between 0.1 and 0.7. Their findings revealed a gradual decrease in system efficiency with an escalating COG recirculation ratio, followed by a more pronounced decline beyond 0.7 due to the low oxygen concentration in the inlet air.

Similar to the studies on AOG recirculation, investigations are also underway concerning the application of COG ejectors. Chan et al. [27] have explored the implementation of a COG ejector for SOFC systems. In their analysis, the electrical efficiency with the ejector configuration reached 65.98%. Notably, they observed that the lower oxygen concentration at the cathode–electrolyte interface resulted in diminished reaction kinetics. This led to a reduction in oxygen concentration at the anode–electrolyte interface, consequently decreasing the chemical potential difference between the anode and cathode when compared to the no recirculation case. Furthermore, the investigation of the SOFC-GT system, incorporating anode and cathode ejectors, has been extended to partial- and full-load conditions. Notably, the system efficiency experiences a variation between 61.8% and 47.7% with a change in the system load. This underscores the need for enhanced performance of ejectors across various load operations, as their stability remains a challenge, warranting further improvement [28].

COG recirculation is under exploration to enhance oxygen utilization and increase heat generation. Elevated COG recirculation rates (greater than 0.5) substantially augment overall oxygen utilization

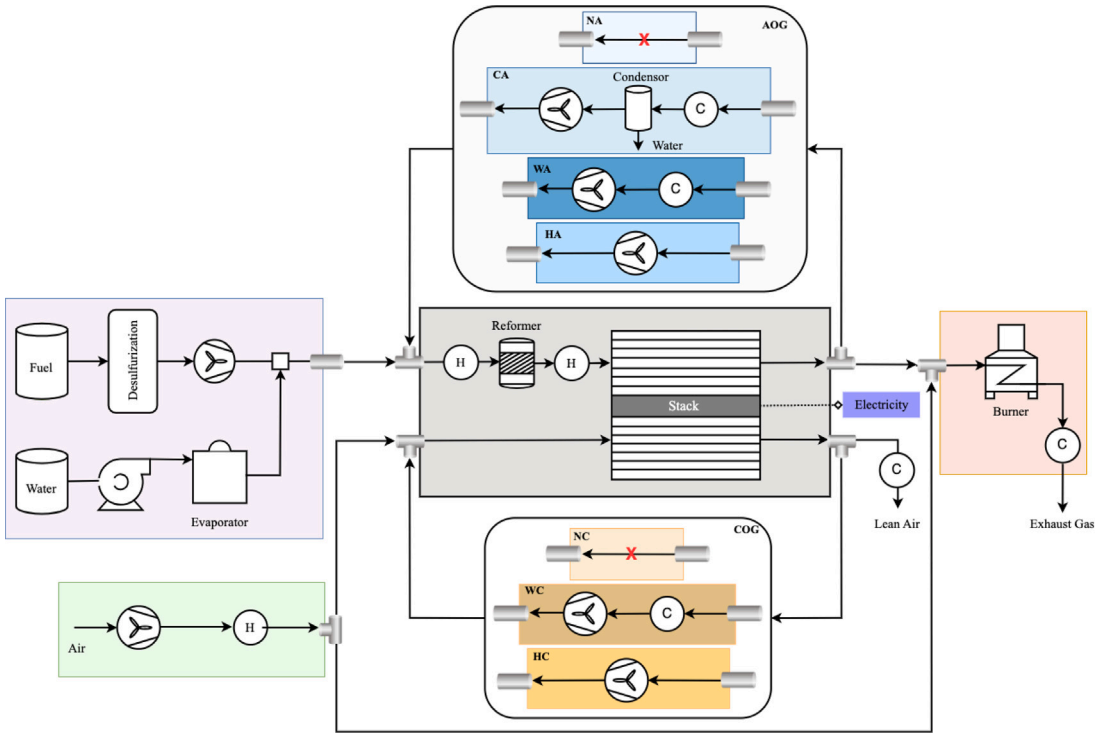

Fig. 1. SOFC System with Different AOG and COG Recirculation.

(exceeding 30%), particularly evident in systems using methane, ammonia and diesel fuels, thereby resulting in an enhancement in heat recovery potential [29]. It is important to note that increasing the COG recirculation leads to lower internal heat recovery, which means that more heat is sent to the exhaust gases [26]. As the COG recirculation ratio rises, the size of the cogeneration system is expanded, and system thermal efficiency is enhanced [30].

While COG recirculation certainly improves thermal performance, it is crucial to maintain a clear perspective on the primary objective (*i.e.*, electricity generation) of the SOFC system. The COG recirculation enhances the overall efficiency of the system. The utilization of COG recirculation should be viewed as an additional benefit, complementing electricity production rather than solely emphasizing heat generation. Balancing thermal improvements with the impact on the system's electrical efficiency is paramount, ensuring that power generation remains at the forefront of consideration.

The prevailing focus of this research has primarily revolved around studying the individual impacts of AOG and COG recirculations, with limited attention directed towards understanding their combined influence. While the pursuit of high system efficiency remains the main objective in energy systems (*e.g.*, SOFC systems), it is imperative to recognize the significance of additional objectives. Ensuring the availability of heat, especially in the context of high-temperature SOFC operations, holds considerable importance. Moreover, the utilization of external water sources introduces added complexity, such as the implementation of a water purification unit. Additionally, there is a noticeable gap in academic research concerning exploring multi-objective optimization methodologies that encompass trade-off solutions considering objectives beyond mere efficiency. This study fills this void by introducing methodologies to analyse the impact of various AOG and COG modules under different operating conditions, offering valuable insights into SOFC system design.

2.3. Objectives and scope of the study

Numerous studies have focused on AOG and COG recirculations, but a comprehensive analysis encompassing all potential cases remains conspicuously absent. Existing research has often focused on specific applications or system layouts, leaving a gap for a holistic examination.

- It becomes essential to gain a profound understanding of the impact of AOG and COG recirculations on the overall performance of the system, including pivotal criteria like electrical efficiency and thermal efficiency.
- This study considers commercially available pressure change equipment, such as high- and low-temperature blowers, for recirculation instead of custom-designed ejectors, which require a specific case-based design rather than standard market purchases.
- Moreover, delving into the favourable conditions for deploying AOG and COG recirculations adds an intriguing dimension. As depicted in Fig. 1, the concept of modularity has been meticulously considered for SOFC systems. The proposed concept divides the SOFC system into six distinct modules, each playing a specific role. These modules encompass fuel and steam preparation, fresh air preparation, pre-reformer and stack, burner, AOG recirculation module, and COG recirculation module.
- The AOG recirculation module has four options: no AOG (NA), cold AOG (CA), warm AOG (WA), and hot AOG (HA). COG recirculation has three options: no COG (NC), warm COG (WC), and hot COG (HC). Through the combination of these diverse modules, a comprehensive landscape unfolds, yielding twelve unique system configurations. While an overarching comparison of these configurations is crucial, a deeper investigation is imperative.
- In this study, the ultimate objective is not merely to determine the best configuration for electrical efficiency, as the optimal solution can vary based on distinct requirements. This exploitative study aims to identify the optimal operational parameters for each configuration while also recognizing their individual advantages and limitations. This information will be useful to industrial manufacturers in making informed decisions regarding module combinations based on specific needs.
- Apart from system electricity efficiency, this study also analyses the availability of waste heat (suitable for industrial applications)

and the valorization of waste heat using a Rankine cycle to produce additional electricity.

3. SOFC system modelling and optimization problem formulation

3.1. SOFC system modelling

The SOFC system has been modelled in Aspen Plus flow sheeting software, which has several modules, including fuel processing module, steam production module, stack with external reformer module, air processing module, combustion module, AOG recirculation module, and COG recirculation module.

Fig. 1 presents all the modules of the SOFC system and also the process connections among these modules. Fuel treated by a desulphurization unit is mixed with heated water/steam via an evaporator. This mixture is heated to the required temperature for the external reformer. Following this, the downstream gas is heated and directed to the anode inlet of the stack, where chemical energy is converted into electrical energy. The anode outlet flow is divided into two streams. One stream is redirected to the inlet of the reformer, having three choices for AOG recirculation: cooling to partially condense the water and compression via a low-temperature AOG blower (cold AOG); direct cooling to the necessary temperature for low-temperature AOG blower without water condensation (warm AOG); or direct compression by a high-temperature AOG blower (hot AOG) for injection into the reformer. The residual anode outlet flow is directed to the burner to ensure full combustion and heat recovery prior to its discharge into the environment.

Fresh air is compressed and heated to the necessary temperature before entering the cathodic side of the stack, where it provides oxygen and regulates stack temperature. The COG referred to as lean air, is then split into two streams. One stream has two options for COG recirculation: either cooling to the temperature required by a low-temperature COG blower (warm COG) or direct compression via a high-temperature COG blower (hot COG). In either option, the COG flow is then mixed with fresh and partially heated air. The remaining COG flow is cooled down before being released into the environment.

It is important to clarify three points. Firstly, within the SOFC system, there is condensed water from cold AOG recirculation downstream of the burner. Condensed water has the potential to reduce fresh water usage. However, in real industrial settings, reusing condensed water poses challenges as it may require a purification unit. Therefore, in this study, condensed water is not reused to avoid the necessity of further complex water purification installations and to simplify the system design.

Secondly, the maximum operating temperature of the burner is set at 900 °C, determined by material resistance considerations. Hence, fresh air is utilized not only to supply oxygen but also to maintain the burner's operating temperature. Indeed, COG also holds the potential to be sent to the burner, where it can provide oxygen for combustion. As the airflow rate is primarily utilized to regulate the stack's operating temperature, it surpasses the flow rate of unconverted fuel. Consequently, only a portion of the COG flow is feasible for maintaining the burner size despite the lower oxygen concentration in COG compared to fresh air, which necessitates a larger burner size compared to using fresh air alone. Moreover, for a modular system design, the COG flow should be used for heat exchange with fresh air. Hence, in this study, COG is directly cooled without being routed to the burner, while fresh air supplies the necessary oxygen for the combustion.

Thirdly, the SOFC system is inherently multifunctional, capable of producing both electricity and waste heat. For selected solutions, two options have been considered to assess the potential of available heat. The first option involves integrating a Rankine cycle (RC), which encompasses regenerative, superheating, reheating, turbine-bleeding, transcritical, and multi-stage cycles, to convert waste heat ranging between 100 and 500 °C into electricity. The detailed methodologies for this approach were developed by Maziar et al. [31,32], which are not presented for brevity reasons. The second option involves evaluating high-quality heat production with a temperature set at 600 °C, suitable for specific industrial processes such as those in the aluminium and glass industry. While it is possible to assess all available heat, including that between 25 and 100 °C, SOFC systems are known for their high-temperature operation compared to other fuel cell systems, such as polymer electrolyte membrane fuel cells and alkaline fuel cells, making it more pertinent to focus on high-temperature heat production capability.

Finally, it is also crucial to grasp the intricacies of modelling the external reformer and stack, as these components are pivotal for the design of the SOFC system.

External reformer: The primary function of the reformer is to transform a portion of the methane into syngas. The reformer outlet stream has a mixture composed of unreacted methane and steam, along with generated hydrogen, carbon monoxide, and carbon dioxide. While the intuitive approach might be to maximize methane conversion inside the external reformer, this is not the typical objective in a practical SOFC system. Instead, the focus often shifts towards minimizing the external reforming. This allows higher internal reforming within the stack. As reforming is an endothermic reaction, internal reforming reduces the amount of fresh air needed to maintain the desired operating temperature of the stack. Consequently, less power is consumed by the air blower. In this study, the external reforming ratio and temperature have been considered as decision variables to evaluate their impacts on the system performance, as shown in Table 1. The reformer has two reactions: steam reforming, characterized as a conversion reaction (Eq. 1), and water-gas shift reaction, classified as an equilibrium reaction (Eq. 2).

$$CH_4 + H_2O \rightleftharpoons 3\,H_2 + CO \qquad \Delta H = 206\,kJ/mol \qquad \{1\}$$

$$CO + H_2O \rightleftharpoons H_2 + CO_2 \qquad \Delta H = -41\,kJ/mol \qquad \{2\}$$

SOFC stack: The SOFC stack model was developed based on the published research studies. The modelling procedure has been outlined and validated in Wang et al. [33] and EU project [34]. As the key focus of this study does not lie in model validation, it is not presented in this research study. The anode and cathode reactions have been presented below (Eqs. 3, 4, 5). Once stack input data is available, area-specific resistance (ASR) can be derived from the current–voltage (I–V) curve obtained from experiments. ASR serves as a critical input for calculating stack power production, which is then compared with experimental values to ensure that the model predictions align with empirical observations. The primary model inputs have been presented in Table 1. The SOFC stack operates in a high single-pass fuel utilization mode, in accordance with the specifications from stack manufacturer [4].

Besides internal reforming reactions (Eqs. 1, 2) that can happen on the anode side, there are also other electrochemical reactions that occur on the anode side:

$$H_2 + O^{2-} \longrightarrow H_2O + 2\,e^- \qquad \{3\}$$

$$CO + O^{2-} \longrightarrow CO_2 + 2\,e^- \qquad \{4\}$$

Cathode reaction:

$$0.5\,O_2 + 2\,e^- \longrightarrow O^{2-} \qquad \{5\}$$

3.2. Multi-objective optimization problem formulation

This study analyses and compares the performance of the SOFC system with twelve different AOG and COG configurations. Table 2 presents a list of objective functions, decision variables with ranges, and constraints with limits. The ranges of decision variables and limits on the constraints have been chosen based on the published research

Table 1
Design and operating specifications of SOFC System; FU: fuel utilization; DV: Decision Variable: LT: Low-Temperature; HT: High-Temperature.

SOFC System	
Stack area	- 3 m^2
Current density	4000 A/cm^2
Stack pressure drop	0.08 bar
Stack temperature difference	70 °C
Stack outlet temperature	750 °C
Stack single-pass FU	0.85
Reformer Operating Conditions	DV
Reformer external reforming ratio	DV
Air blower suction pressure	1 bar
Air blower pressure increase	0.3 bar
Air blower isentropic efficiency	0.8
Air blower mechanical efficiency	0.85
AOG/COG Blower Model Inputs	
LT blower mechanical efficiency	0.85
LT blower isentropic efficiency	0.8
HT blower mechanical efficiency	0.85
HT blower isentropic efficiency	0.8
AOG blower discharge pressure	1.25 bar
COG blower pressure increase	0.2 bar

Table 2
Details of objective functions, decision variables and constraints.

Objective Function (Obj. Fun.)			
EE	Maximum Electrical efficiency, %		
AOG RR	Maximum AOG Recirculation Ratio, -		
EWF	Minimum External Water Flow, mol/s		
AHD	Minimum Air Heater Duty, kW		
Decision Variables with Lower and Upper Limits			
ERT	External Reforming Temperature, °C	510	550
ERR	External Reforming Ratio, -	0.1	0.5
FI	Fuel Input, mol/s	0.017	0.02
EWF	External Water Flow, mol/s	0.01	0.09
AOG RR	AOG Recirculation Ratio	0	0.9
COG RR	COG Recirculation Ratio	0	0.65
AOG CondT	AOG Condensation Temperature, °C	25	95
Constraints with Limits			
S/C Ratio	Greater Than	1.5	
O/C Ratio	Greater Than	2.5	
O_2 in Outlet Air, mol%	Greater Than	15	
DTstack, °C	Less Than	100	
Power Output, kW	Range	9	11

studies on SOFC systems. Several decision variables and their ranges require justification. It is widely acknowledged that the SOFC stack can perform internal reforming, which is favourable for the system design. Steam methane reforming, an endothermic reaction, can utilize the heat within the stack, thereby reducing the need for air on the cathode side and subsequently lowering air blower power consumption. However, the stack used in this study can only achieve a maximum of 90% internal reforming according to the manufacturer, necessitating at least 10% external reforming in the external reformer. Consequently, the External Reforming Ratio (ERR) has been set between 0.1 and 0.5. According to the published research study [35], achieving such ERR typically requires a reforming temperature ranging from 510 to 550 °C, which has been designated as the operating temperature range for the external reformer (ERT).

For each configuration, Table 3 presents objective functions and decision variables. For all configurations, maximum electrical efficiency is always one of the objective functions. Further, configurations without AOG recirculation (NCNA, WCNA, and HCNA) have two objective functions, whereas all other configurations have three objective functions. Four decision variables, namely external reforming temperature, external reforming ratio, fuel input and external water flow, are common in

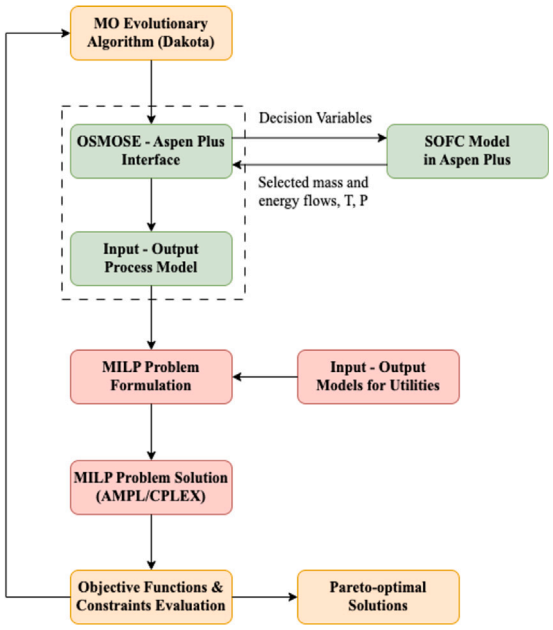

Fig. 2. Working Principle of OSMOSE: A Tool for Process Integration and Optimization.

the optimization problems for all configurations. The AOG recirculation ratio has been used as a decision variable for configurations with cold, warm, and hot AOG recirculations, whereas the COG recirculation ratio has been used as a decision variable for configurations with warm and hot COG recirculations.

The formulated multi-objective optimization problems have been solved using OSMOSE, which is an in-house decision-making tool developed by our research group. Fig. 2 presents a simple flowchart of the OSMOSE working principle. OSMOSE can be used to perform multi-objective optimization, heat integration, multi-period optimization and scenario analysis. It can also use process models, utility models, cost models, and environmental impact models to compute key performance indicators that can be used by decision-makers. OSMOSE can be linked with external multi-objective optimization tools (such as Dakota) to solve an optimization problem. To optimize the performance of a process that has been modelled in a flow sheeting software, OSMOSE is linked with external software for transferring the values of decision variables and recovering important data from the process model. To perform the process and heat integration, OSMOSE formulates a mixed integer linear programming (MILP) problem using process models and utility models to achieve optimal interconnections and mass and heat flows. The MILP problem is solved using the AMPL/CPLEX solver. Finally, OSMOSE presents optimum results for objective functions, decision variables, selections or sizes of utilities, and also different types of heat curves.

4. Results and discussion

This study analyses and compares the performance of twelve AOG and COG configurations. The comparison has been conducted, both collectively and individually, by selecting some representative solutions. Initially, the optimization outcomes for all system configurations are presented to gain insights into their layout capabilities across diverse objective functions. Subsequently, the performance of COG recirculation systems, encompassing options of no COG, warm COG, and hot COG, is presented. Finally, the performance of AOG recirculation systems is discussed, including instances of no AOG, cold AOG, warm AOG, and hot AOG.

Table 3
SOFC system with different AOG and COG configurations.

Configurations			Obj. Fun.				Decision Variables						
Name	COG	AOG	EE	AOG RR	EWF	AHD	ERT	ERR	FI	EWF	AOG RR	COG RR	AOG CondT
NANC	No	No	x		x		x	x	x	x			
NCCA	No	Cold	x	x	x		x	x	x	x	x		x
NCWA	No	Warm	x	x	x		x	x	x	x	x		
NCHA	No	Hot	x	x	x		x	x	x	x	x		
WCNA	Warm	No	x			x	x	x	x	x		x	
WCCA	Warm	Cold	x	x		x	x	x	x	x	x	x	x
WCWA	Warm	Warm	x	x		x	x	x	x	x	x	x	
WCHA	Warm	Hot	x	x		x	x	x	x	x	x	x	
HCNA	Hot	No	x			x	x	x	x	x		x	
HCCA	Hot	Cold	x	x		x	x	x	x	x	x	x	x
HCWA	Hot	Warm	x	x		x	x	x	x	x	x	x	
HCHA	Hot	Hot	x	x		x	x	x	x	x	x	x	

4.1. Comparative analysis of all configurations

As depicted in Fig. 3(a), the optimized results for twelve system configurations are graphed for the system's electrical efficiency. The base case denoted as NCNA (no COG and no AOG), serves as the benchmark. The optimum electrical efficiency of the base case has a range spanning from 65% to nearly 72%, contingent upon adjustments in the decision variables. After the analysis of other configurations,

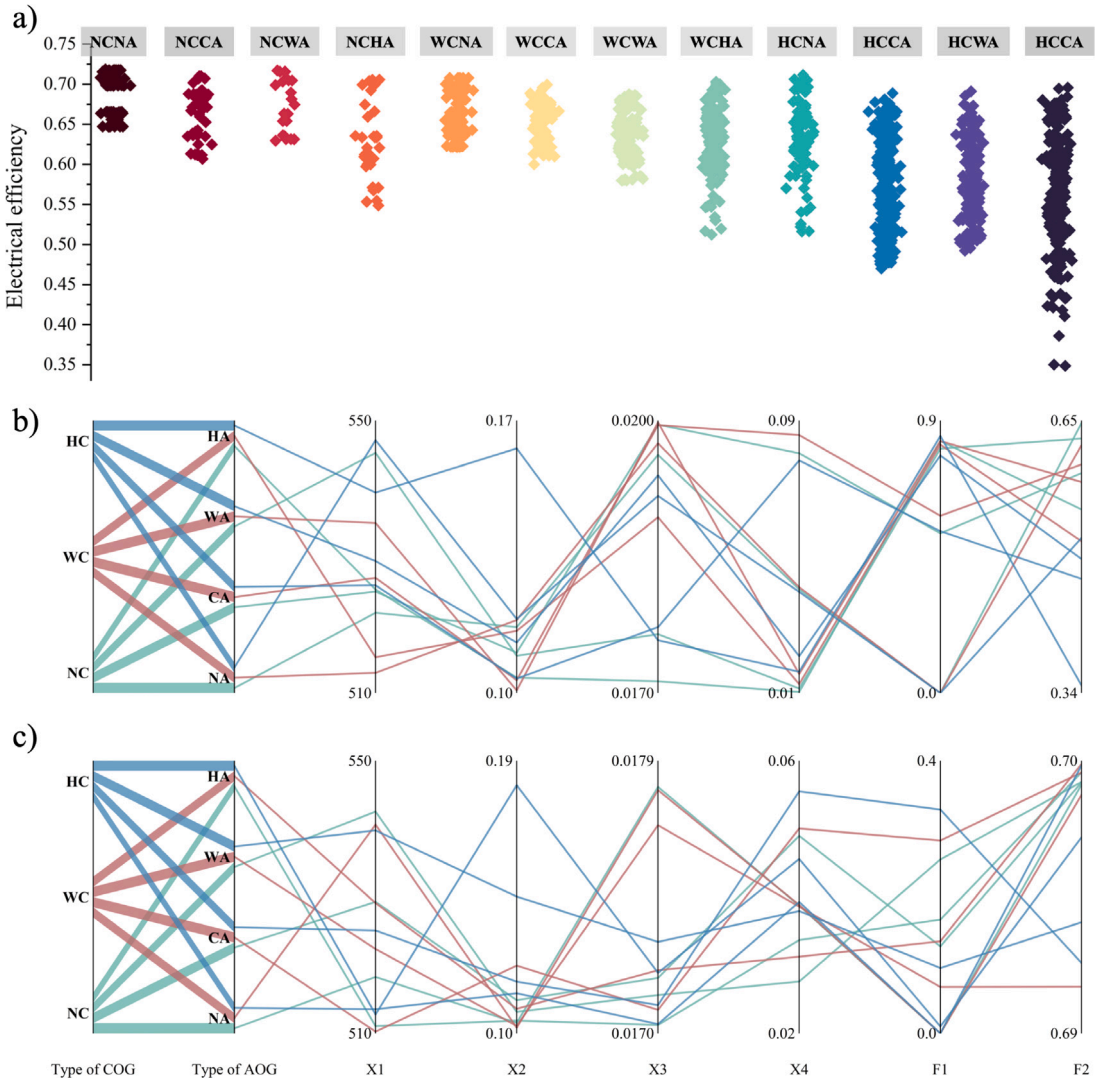

Fig. 3. Performance Analysis of twelve Configurations: (a) All Solutions with Electrical Efficiency, (b) Solutions with Minimum Electrical Efficiency, and (c) Solutions with Maximum Electrical Efficiency. F1 — AOG Recirculation Ratio, F2 — Electrical Efficiency, X1 — External Reforming Temperature (°C), X2 — External Reforming Ratio, X3 — Fuel Input (mol/s), X4 — External Water Flow (mol/s).

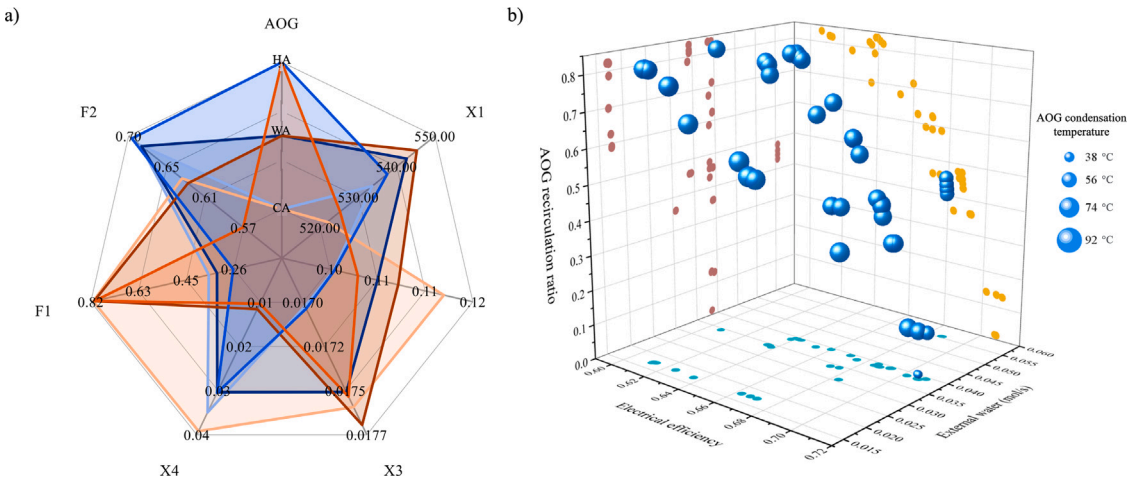

Fig. 4. (a) Six Representative Solutions from Optimization Results for No COG (NC) with Different AOG Recirculation; F1 — AOG Recirculation Ratio, F2 — Electrical Efficiency, X1 — External Reforming Temperature (°C), X2 — External Reforming Ratio, X3 — Fuel Input (mol/s), X4 — External Water Flow (mol/s), and (b) Impact of CA Condensation Temperature on Three Objective Functions, for NCCA Layout.

a salient observation materializes: all configurations manifest the capacity to achieve similar levels of electrical efficiency as the base case. A significant disparity in electrical efficiency becomes evident in certain cases, namely NCHA, WCHA, HCNA, HCCA, HCWA, and HCHA. The observed discrepancy highlights the inter-correlation of objective functions, particularly those related to external water flow rate and air heater duty, impacting the system's overall efficiency. It is noteworthy to note the impact of AOG/COG recirculation on electrical efficiency, especially in the case of HCHA. In this case, the minimum achievable electrical efficiency can plummet to 35%, with simultaneous optimization of the other two objective functions. It becomes evident that, for certain cases, the potential to attain the highest electrical efficiency akin to the base case is not feasible. For instance, configurations like WCWA, HCCA, HCWA and HCCA have limitations in achieving electrical efficiency, with the maximum electrical efficiency plateauing at about 70%.

It is equally crucial to comprehend the specific decision variables and their impact on the performance of different configurations. This insight aids in discerning the nature of this influence, and it is presented in Figs. 3(b) and (c), where solutions with minimum and maximum electrical efficiency are depicted. An additional objective function, the maximum AOG recirculation ratio, is considered for all cases except those involving no AOG (*i.e.*, NCNA, WCNA, and HCNA). In the case of minimum electrical efficiency, a substantial range spanning from 35% to 65% is observed, contingent upon the specific configuration. The SOFC system exhibits no particular preference for ERT, as evident by the positions of different lines. This implies that ERT lacks sensitivity concerning the objectives being pursued. In the optimization problem, the second decision variable (*i.e.*, ERR) is bounded between 0.1 and 0.5. The plot illustrates an interesting trend: a lower ERR corresponds to the improved performance of the SOFC system. Notably, the maximum ERR achieved is only around 0.18 or below for all the cases in Figs. 3(b) and (c), significantly below the upper limit of this decision variable. This outcome is indeed logical, as a lower ERR implies a greater emphasis on the internal reforming inside the stack. As internal reforming involves an endothermic reaction, an elevated degree of reaction requires less air for cooling and a reduction in the air blower's power consumption.

An intriguing analysis emerges from examining the interplay between fuel input, external water flow, AOG recirculation ratio (for cases without AOG) and electrical efficiency. Fuel input and AOG recirculation are two factors deeply connected with system fuel utilization (FU). A high value of system/global FU leads to better performance. Electricity generation does not increase linearly with fuel energy input when considering a fixed stack size. This mechanism is a key factor behind the cases with minimum electrical efficiency, as depicted in Fig. 3(b). Further, when the system has a large AOG flow, the demand for external water flow diminishes. This explains the trend observed for external water flow, where the majority of the lines are close to the lower limit (0.01 mol/s). The system still needs water flow from outside because of the constraints (S/C and O/C ratios) in the optimization formulation, which are meant to prevent carbon deposition. As anticipated, the HCHA case exhibits poor performance based on electrical efficiency. The high AOG recirculation in this case, coupled with substantial fuel utilization, results in a detrimental effect on electrical efficiency due to the AOG blower power consumption.

As the cases aiming for optimal electrical efficiency are examined (Fig. 3c), a consistent pattern emerges across all cases except those associated with no AOG. In these cases, a common trend requires low AOG recirculation to attain the utmost efficiency. This contrast becomes evident when comparing the maximum AOG recirculation ratios (0.9 versus 0.35) depicted in Figs. 3(b) and (c). However, achieving higher global FU necessitates an increase in AOG recirculation and a corresponding reduction in fuel input. This is a key reason for numerous cases converging towards the lower limit of 0.017 mol/s for fuel input. Generally, a modest amount of AOG recirculation contributes positively to electrical efficiency and external water conservation. Nevertheless, it is essential to strike a balance, as excessive AOG recirculation can lead to adverse effects on system performance.

4.2. Impact of AOG recirculation on SOFC system performance

This sub-section evaluates the performance of the SOFC system for different AOG recirculations with fixed COG recirculation: no COG with different AOG, warm COG with different AOG, and hot COG with different AOG.

The spider plot is employed to illustrate six optimum solutions. Within these selected solutions, three instances highlight high AOG recirculation ratios (F1), depicted in varying shades of orange. Conversely, the other three solutions demonstrate low AOG recirculation ratios, depicted in shades of blue (see Fig. 4(a)).

The spider plot categorizes six optimum solutions into two groups based on the AOG recirculation ratio — low and high. Each group is evaluated regarding different decision variables, such as recirculation type, and their collective impact on another critical objective function: system efficiency (F2). This visual representation is designed to illustrate how variations in decision variables influence effectiveness levels, thereby highlighting the sensitivity of system efficiency to these factors, which enables potential industrial partners to visualize and

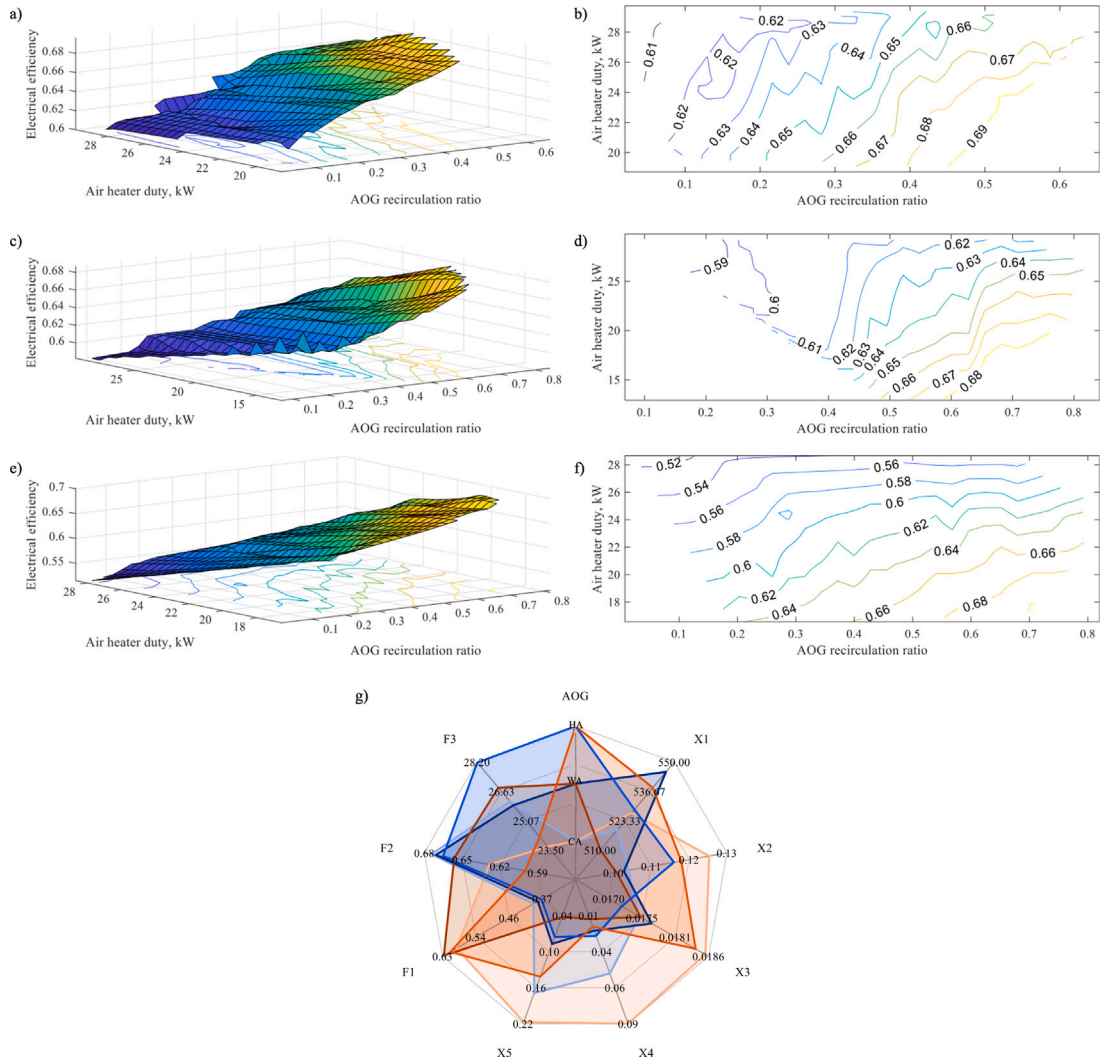

Fig. 5. SOFC System Performance for (a, b) WCCA, (c, d) WCWA, and (e, f) WCHA Configurations. (g) Six Representative Solutions from Optimization Results for Warm COG (WC) with Different AOG Recirculation; F1 — AOG Recirculation Ratio, F2 — Electrical Efficiency, F3 — Air Heater Duty (kW), X1 — External Reforming Temperature (°C), X2 — External Reforming Ratio, X3 — Fuel Input (mol/s), X4 — External Water Flow (mol/s).

comprehend the complex interplay between decision-making variables and their consequent effects on overall performance.

No COG with different AOG: As illustrated in Fig. 4(a), six distinct optimized solutions have been chosen for detailed analysis. Three solutions are characterized by a low AOG recirculation ratio (F1, about 0.25 to 0.4), while the remaining three solutions exhibit high AOG recirculation ratios (about 0.82). Evidently, instances with low AOG recirculation ratios consistently manifest higher electrical efficiency (F2) values while having similar fuel inputs (X3), thus corroborating the findings from the preceding sub-section. However, Fig. 4(a) unveils a noteworthy observation: for CA configurations, system efficiency surpasses that of configurations utilizing WA and significantly outperforms those employing HA configurations. This trend becomes even more pronounced with increased AOG recirculation. Notably, the efficiency gain comes at the expense of elevated external water flow, potentially four times higher than that required by WA and HA configurations. This disparity is primarily attributed to the exponential increase in AOG blower power consumption. Additionally, it is important to note that the efficiency of the AOG blower at elevated temperatures is considerably diminished, further contributing to the observed trends.

In the NCCA case, an additional decision variable, AOG condensation temperature, comes into play. Fig. 4(b) illustrates the relationship between the condensation temperature and three objective functions through a 3D bubble plot, where smaller bubble sizes correspond to lower temperatures. The optimum condensation temperature typically falls within the range of 60 to 80 °C. This alignment arises due to the optimization limits governing the AOG recirculation ratio and external water flow. As anticipated, the highest efficiency emerges for the solutions where water condensation can be fully achieved at 38 °C, albeit at the cost of the highest external water flow. It is worth noting that the projection on the XZ plane, namely the yellow scatter points, demonstrates that once a certain AOG recirculation ratio is exceeded, additional increases in AOG recirculation do not result in significant improvements in efficiency. This observation is in perfect agreement with the preceding arguments.

Warm COG with different AOG: Moving on to WC configurations, the analysis encompasses three primary objectives: electrical efficiency, air heater duty, and AOG recirculation ratio. Fig. 5 illustrates the optimized results for WCCA (plots a and b), WCWA (plots c and d), and WCHA (plots e and f) configurations. A comparative assessment of these three configurations reveals noteworthy observations. Upon comparison, it becomes evident that WCCA consistently exhibits higher electrical efficiency, aligning with expectations. This conclusion echoes the findings established in the preceding sub-section. Notably, it is discernible that the minimum attainable electrical efficiencies for the three configurations (WCCA, WCWA, and WCHA) are 0.61, 0.59, and

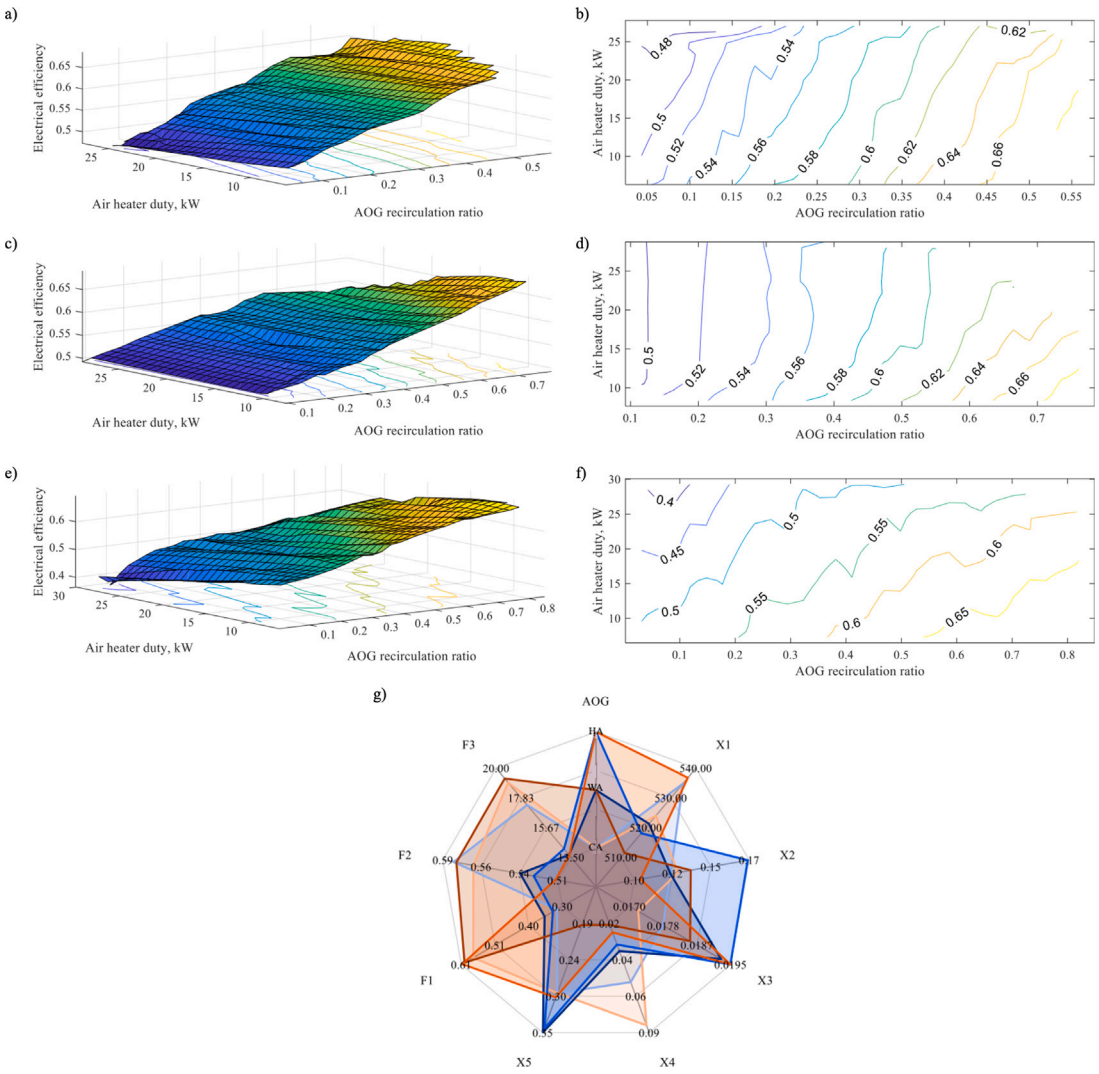

Fig. 6. SOFC System Performance for (a, b) HCCA, (c, d) HCWA, and (e, f) HCHA Configurations. (g) Six Representative Solutions from Optimization Results for Hot COG (HC) with Different AOG Recirculation; F1 — AOG Recirculation Ratio, F2 — Electrical Efficiency, F3 — Air Heater Duty (kW), X1 — External Reforming Temperature (°C), X2 — External Reforming Ratio, X3 — Fuel Input (mol/s), X4 — External Water Flow (mol/s).

0.52, respectively. This disparity arises due to a decline in blower efficiency with an increase in the inlet flow temperature. However, despite these differences, all three configurations retain the potential to achieve identical efficiency by varying different decision variables. This assertion finds validation in the examination of decision variable values for the three configurations, as depicted in Fig. 5(g).

Fig. 5(g) reaffirms a similar conclusion as Fig. 4(a). However, there is a distinct trend in Fig. 5(g), which diverges from the previous findings. Notably, WCWA exhibits higher efficiency compared to WCCA. This shift can be attributed primarily to the lower COG recirculation ratio that WCWA employs in contrast to WCCA (80% less). A more detailed exploration of this trend will be undertaken later in this study.

Hot COG with Different AOG: The final analysis in this section pertains to hot COG with different AOG. As shown in Fig. 6, all the optimization results consistently align with the above-presented optimization results. A comparative examination of Figs. 4, 5, and 6 confirms a shift in the electrical efficiency of the system. This decline is attributable to the temperature of COG flow, a topic that will be thoroughly analysed in the following section.

In summary, the analysis presented in this part focuses on assessing the effects of varying AOG recirculation temperature, flow, and composition. Key findings encompass the impact of AOG recirculation on system efficiency and the significance of condensation temperature within specific contexts. Comparative evaluations across cold AOG, warm AOG, and hot AOG configurations reveal distinct efficiency trends. Notably, cold AOG exhibits superior efficiency performance, albeit with a higher external water flow. Conversely, hot AOG showcases inferior efficiency performance, which is attributed to reduced AOG blower efficiency at elevated temperatures. However, it is imperative to note that these conclusions do not account for available heat within the system. Consequently, the system's overall efficiency may not necessarily align with the observed electrical efficiency. The analyses yield valuable insights into the complex interplay of system performance factors under diverse conditions and establish a groundwork for the subsequent analysis.

4.3. Impact of COG recirculation on system performance

This sub-section analyses the performance of three COG recirculation options: no COG, warm COG, and hot COG. There are three objective functions, namely electricity efficiency, air heater duty, and AOG recirculation ratio. The optimization problem formulation also includes the COG recirculation ratio as a decision variable, in addition to the standard set of decision variables.

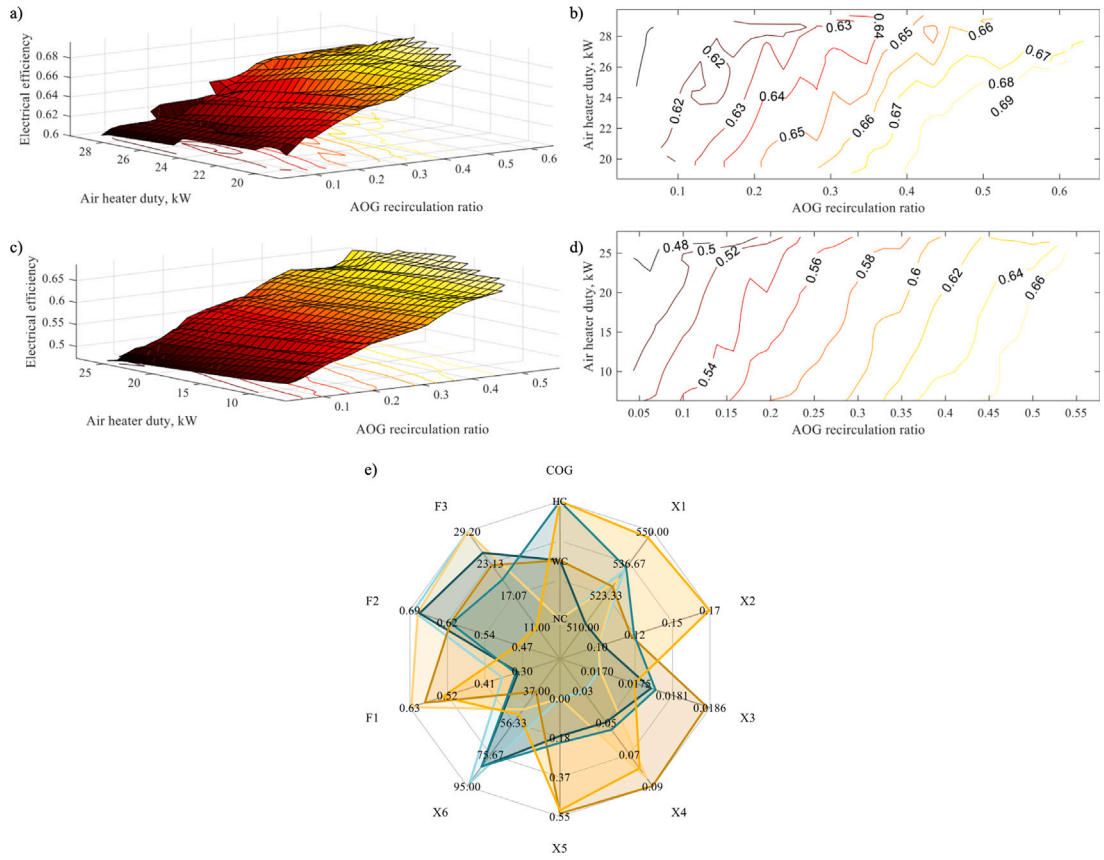

Fig. 7. SOFC System Performance for (a, b) WCCA, and (c, d) HCCA Configurations. (e) Six Representative Solutions from Optimization Results for Cold AOG (CA) with Different AOG Recirculation; F1 — AOG Recirculation Ratio, F2 — Electrical Efficiency, F3 — Air Heater Duty (kW), X1 — External Reforming Temperature (°C), X2 — External Reforming Ratio, X3 — Fuel Input (mol/s), X4 — External Water Flow (mol/s), X5 — COG Recirculation Ratio, X6 — AOG Condensation Temperature.

Similar to the AOG analysis, the spider plot is also employed to illustrate six optimum solutions. Within these selected solutions, three instances have high COG recirculation ratios (F1), depicted in varying shades of yellow. Conversely, the other three instances demonstrate low COG recirculation ratios, depicted in shades of turquoise (see Fig. 7e).

Cold AOG with Different COG: Three distinct system configurations have been examined: NCCA, WCCA, and HCCA. In the case of the NCCA configuration, minimizing air heater duty as an objective function is not applicable, and therefore, it is not presented in the 3D plot. For WCCA configuration, as depicted in Figs. 7(a) and (b), the system efficiency fluctuates between 0.61 and 0.69. Conversely, for HCCA configuration, as illustrated in Figs. 7(c) and (d), system efficiency varies between 0.48 and 0.66. This observation indicates that when replacing WC with HC, the system efficiency consistently shifts to a lower range. This outcome can primarily be attributed to the considerably diminished efficiency of COG blowers at elevated temperatures. Additionally, the advantages of employing HC are evident in Fig. 7(d), where the minimum air heater duty can drop below 10 kW. This reduction indirectly enhances the availability of heat within the system. Conversely, for the WC case, the minimum air heater duty has a value of about 20 kW.

Fig. 7(e) provides a comprehensive view of the effects of different decision variables on the objective functions. This figure shows six optimized solutions grouped into two categories: those associated with high AOG recirculation ratios (shown in yellow) and low AOG recirculation ratios (shown in turquoise). Notably, the NCCA configuration consistently demonstrates the highest system efficiency across low and high AOG recirculation ratios. Interestingly, the WCCA configuration also exhibits relatively high system efficiency in specific instances when the COG recirculation ratio is around 0.18, and the AOG recirculation ratio is around 0.3. Further, the WCCA configuration also shows relatively low external water usage, which is mainly due to the partial condensation of cold AOG recirculation. Conversely, hot COG configuration consistently results in lower system efficiency. For instance, with a 55% COG recirculation ratio, when combined with the impacts of other decision variables, the system efficiency can drop to 47%. However, it is worth noting that such cases experience a substantial reduction in air heater duty, reaching a value of about 11 kW. After thorough analysis, it becomes evident that the WCCA configuration retains the potential to achieve system efficiency comparable to the NCCA configuration by leveraging collaborative interactions with other decision variables.

Warm AOG with Different COG: Fig. 8 presents a comprehensive overview of all COG cases (NCWA, WCWA, HCWA) incorporating warm AOG. In the NCWA configuration, minimizing air heater duty is irrelevant, so it is not shown in the 3D plot. Specifically, Figs. 8(a) and (b) illustrate all optimum solutions obtained for WCWA configuration. Notably, the system efficiency varies from 0.6 to 0.68, with the potential for a minimum air heater duty of around 15 kW. Transitioning to the HCWA configuration, as anticipated, Figs. 8(c) and (d) reveal a shift towards lower system efficiency (varying between 0.5 and 0.66) while also showcasing the possibility of achieving a minimum air heater duty of as low as 10 kW. These observations align with the conclusions drawn previously. Further, focusing on the analysis of decision variables (Fig. 8e), it is evident that NCWA configuration exhibits the highest electrical efficiency, while WCWA configuration

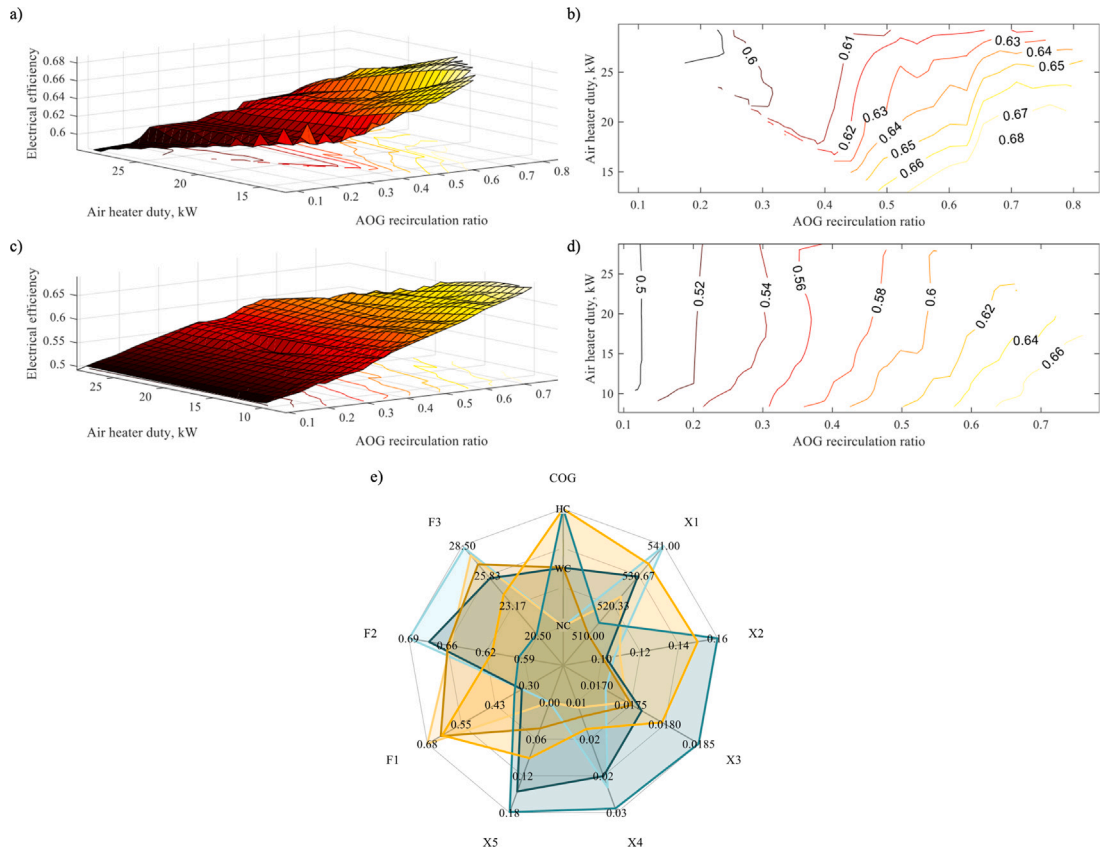

Fig. 8. SOFC System Performance for (a, b) WCWA, and (c, d) HCWA Configurations. (e) Six Representative Solutions from Optimization Results for Warm AOG (WA) with Different AOG Recirculation; F1 — AOG Recirculation Ratio, F2 — Electrical Efficiency, F3 — Air Heater Duty (kW), X1 — External Reforming Temperature (°C), X2 — External Reforming Ratio, X3 — Fuel Input (mol/s), X4 — External Water Flow (mol/s), X5 — COG Recirculation Ratio.

remains competitive, particularly through an appropriate warm COG recirculation.

Hot AOG with Different COG: The optimization results for configurations involving hot AOG recirculation with three COG recirculation (NCHA, WCHA, HCHA) are presented in Fig. 9. In the NCHA configuration, minimizing air heater duty as an objective function is not applicable; thus, it is omitted from the 3D plot. Upon closer analysis of the WCHA layout presented in Figs. 9(a) and (b), it becomes evident that system efficiency varies between 0.54 and 0.68. Further, there exists a possibility for a minimum air heater duty of about 18 kW. Shifting focus to HCHA optimization results (Figs. 9(c) and (d)), it can be observed that these particular solutions demonstrate a range of electrical efficiency between 0.4 and 0.65, along with a potential minimum air heater duty of less than 10 kW. Fig. 9(e) does not introduce any new distinct insights, as the depicted aspects have been previously discussed. However, an intriguing observation arises when comparing Figs. 7, 8, and 9. Despite the different types of AOG involved, the system can perform similarly when all decision variables are adjusted.

In this detailed analysis, various COG recirculation options have been systematically explored, with a focus on their impacts on system performance. Each configuration has been evaluated based on objective functions such as electrical efficiency, air heater duty, and the AOG recirculation ratio. The influence of the COG recirculation ratio, a unique decision variable, was also considered in the optimization process. Despite additional power consumption by the COG blower, the warm COG configuration shows competitive results when compared to the no COG configuration. Additionally, configurations that incorporate hot COG exhibit lower efficiency due to the diminished electrical efficiency of the COG blower at elevated temperatures. However, this configuration also presents a noteworthy advantage in terms of increasing the available heat within the SOFC system. Comparing the three types of AOG recirculation in the analyses, it became apparent that regardless of the AOG type, the system performance remained consistent when all decision variables were manipulated.

4.4. Heat integration of the SOFC system

AOG/COG recirculation can potentially cause changes in the system's thermal efficiency. Therefore, this section is devoted to a thorough analysis of the heat performance of the system.

In accordance with Fig. 10, process flow diagrams have been developed for twelve distinct cases and configurations. These diagrams include various modules, heaters, and coolers, as presented in Fig. 1. The fuel undergoes heating in the heater (H1), while water is converted into steam by using the heater (H2), evaporator (H3), and superheater (H4). Subsequently, fuel and steam are mixed with the recycled AOG stream if the AOG line has been activated. This combined flow is then subjected to heating or cooling via H5 or C5 before proceeding to the external reformer. As reforming is an endothermic reaction, the external reformer has to be heated (H6) to maintain the reforming temperature. After external reforming, the reformate gases are directed to the stack for the conversion of chemical energy into electricity. Conversely, fresh air is heated (H8) to the required temperature, subsequently mixing with the recycled COG stream if the COG line has been activated. The resultant air mixture proceeds through the heater (H8') and enters the stack as part of the overall conversion process. The fresh air flow rate is manipulated as the stack outlet temperature should be maintained at 750 °C. At SOFC downstream, a portion of AOG can be diverted for recirculation while the remaining AOG is directed to a burner. This burner is required to combust any unconverted fuel, utilizing oxygen supplied by the fresh air. Subsequently, coolers C1

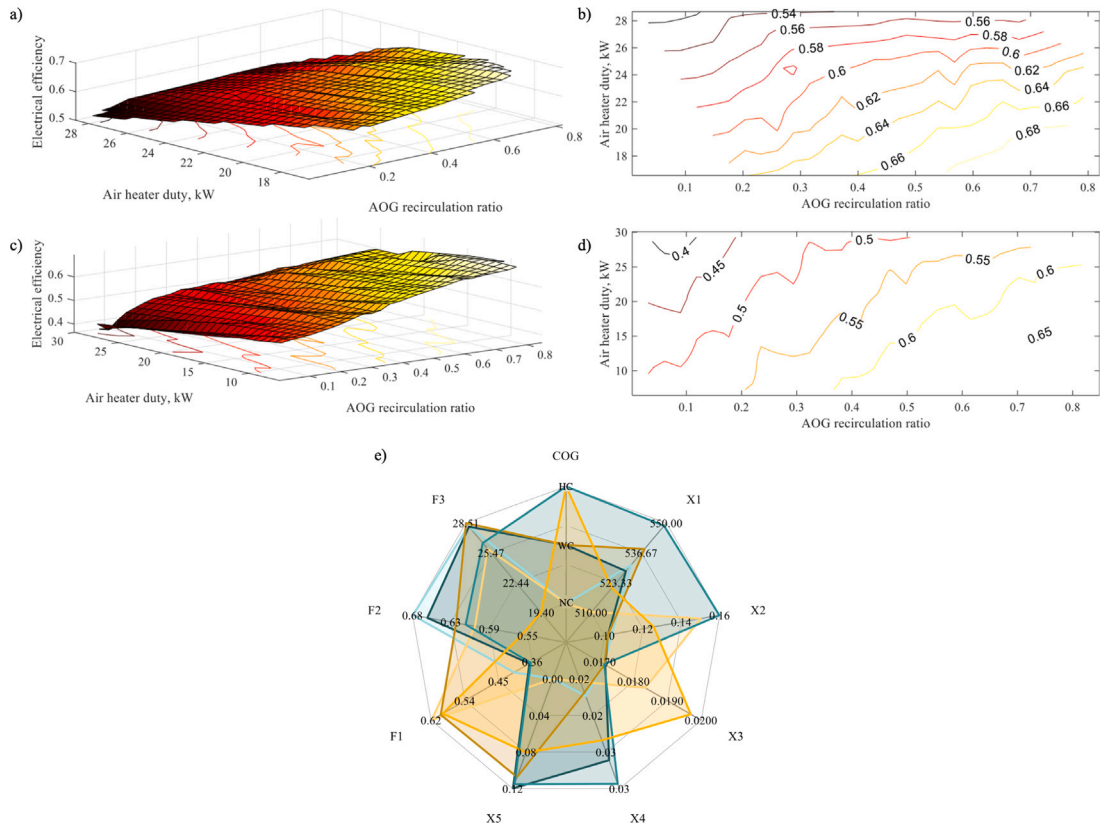

Fig. 9. SOFC System Performance for (a, b) WCHA, and (c, d) HCHA Configurations. (e) Six Representative Solutions from Optimization Results for Hot AOG (HA) with Different AOG Recirculation; F1 — AOG Recirculation Ratio, F2 — Electrical Efficiency, F3 — Air Heater Duty (kW), X1 — External Reforming Temperature (°C), X2 — External Reforming Ratio, X3 — Fuel Input (mol/s), X4 — External Water Flow (mol/s), X5 — COG Recirculation Ratio.

and C2 are utilized to reduce the temperature of the combustion gases. The fresh air flow rate is determined in such a way that it ensures the maximum temperature inside the burner (less than 900 °C) based on the market availability of the burner.

For cold AOG recirculation, AOG flow needs to undergo a two-stage cooling process. Initially, it is cooled to water condensation temperature in a cooler (C3'_1). Subsequently, AOG flow is further cooled (C3'_2) to an optimized temperature for partial water condensation.

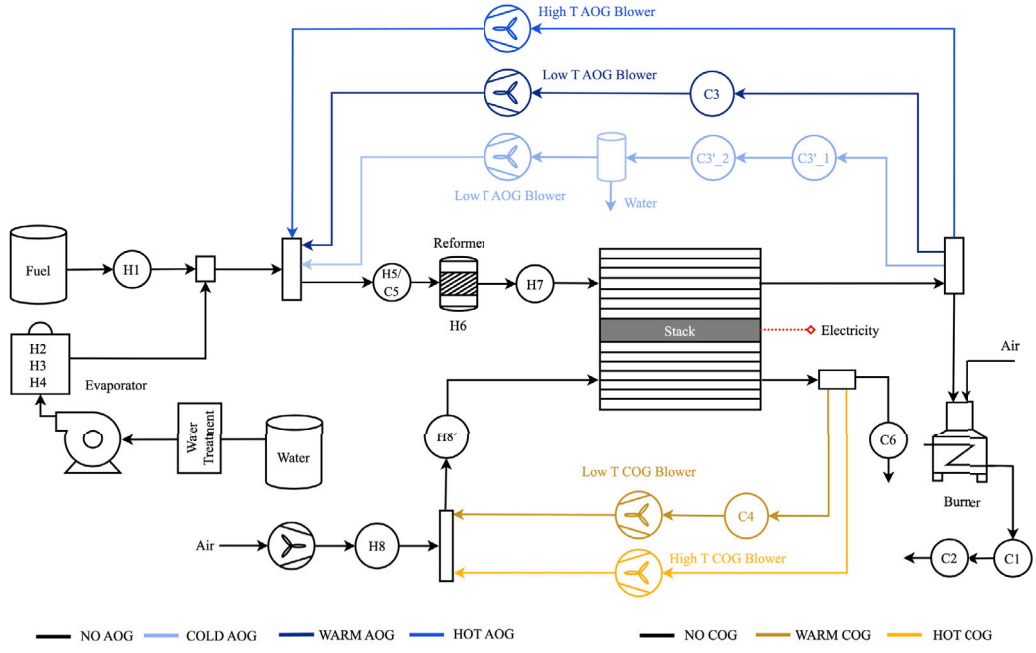

Fig. 10. SOFC System Process Flow Diagram with Various AOG and COG Recirculation; Different Connections will be Activated/Deactivated for Different Cases.

Table 4
Optimized results for twelve selected solutions (One from Each Case) with identical fuel input and comparable electrical efficiency.

	NCNA	NCCA	NCWA	NCHA	WCNA	WCCA	WCWA	WCHA	HCNA	HCCA	HCWA	HCHA
Fuel input, mole/s	0.0175	0.0175	0.0175	0.0175	0.0175	0.0175	0.0175	0.0175	0.0175	0.0175	0.0175	0.0175
External water flow, mole/s	0.086	0.039	0.013	0.022	0.048	0.089	0.024	0.031	0.037	0.058	0.036	0.033
Fresh air input, mole/s	1.616	1.396	1.369	1.387	0.602	1.233	0.75	1.238	1.025	1.36	1.188	1.287
Fresh air blower power, kW	0.50	0.43	0.43	0.43	0.19	0.38	0.23	0.39	0.32	0.41	0.37	0.40
AOG recirculation flow, mole/s	0	0.137	0.136	0.08	0	0.081	0.037	0.052	0	0.079	0.01	0.033
AOG blower power, kW	0	0.10	0.13	0.35	0	0.02	0.03	0.24	0	0.04	0.01	0.15
COG recirculation flow, mole/s	0	0	0	0	0.889	0.176	0.669	0.167	0.259	0.071	0.199	0.084
COG blower power, kW	0	0	0	0	0.78	0.16	0.59	0.15	0.95	0.26	0.73	0.31
Electricity from stack, kW	9.69	9.71	9.72	9.84	10.02	9.74	10.04	9.87	10.29	9.82	10.15	9.97
Fuel input energy, kW	14.04	14.04	14.04	14.04	14.04	14.04	14.04	14.04	14.04	14.04	14.04	14.04
Net electricity from system, kW	9.19	9.18	9.17	9.06	9.05	9.19	9.19	9.10	9.02	9.11	9.04	9.11
DC electrical efficiency, %	65.4	65.4	65.3	64.5	64.5	65.4	65.4	64.8	64.3	64.9	64.4	64.9
Fresh air to burner, mole/s	0.009	0.018	0.018	0.016	0.009	0.014	0.015	0.014	0.012	0.013	0.012	0.016
Minimum number of heat exchangers	14	16	15	14	15	18	16	15	14	16	15	14
Total area of heat exchangers, m^2	1.89	1.27	1.16	1.13	1.17	1.80	1.07	1.17	0.79	1.20	0.94	1.44
Cold utility, kW	6.57	6.21	6.33	6.34	6.34	6.25	6.23	6.31	6.14	6.20	6.14	6.26
Availability of high quality heat and waste heat valorization												
High quality heat (600 °C), kW	0.71	2.43	3.45	2.94	1.32	0.16	2.20	2.64	2.60	1.73	2.65	2.71
Thermal efficiency, %	5.0	17.3	24.6	20.9	9.4	1.2	15.7	18.8	18.5	12.3	18.8	19.3
RC electricity generation, kW	0.72	1.66	1.86	1.80	1.36	0.17	1.65	1.65	1.72	1.56	1.73	1.53
RC electrical efficiency, %	5.1	11.8	13.3	12.8	9.7	1.2	11.8	11.8	12.3	11.1	12.3	10.9

In the case of warm AOG recirculation, AOG flow only requires cooling to a temperature of about 120 °C. This temperature aligns with the common design temperature for low-temperature blowers. In COG recirculation cases, the positioning of heaters or coolers has been carefully selected to optimize heat utilization within the system. For instance, in the case of hot COG, heater H8 plays a crucial role. It heats the fresh air to a specific temperature before mixing it with the high-temperature COG flow. This approach ensures that the mixed air temperature effectively reaches the stack's operating temperature. In the hot COG case, heater H8 is activated, while heater H8' remains inactive. This choice is made to avoid mixing cold fresh air with high-temperature COG flow, resulting in inefficient use of the high-quality heat and potentially necessitating additional heat supply via heater H8'. Conversely, in the case of warm COG recirculation, it is more sensible to mix the warm COG flow with fresh air first. Subsequently, the mixed flow is heated to the stack inlet temperature in the heater (H8'). If the same approach were used for hot and warm COG recirculation, the outlet temperature of H8 could become excessively high for a warm AOG case, leading to the requirement for expensive materials that can withstand such high temperatures and potentially necessitating additional hot utility.

As depicted in Fig. 3, various layouts can yield comparable electrical efficiencies. To ensure a fair comparison of heat performance across all cases, twelve solutions with a similar DC electrical efficiency of approximately 65% and the same optimized fuel input flow rate (0.0175 mole/s) have been selected. The results for the twelve chosen solutions are summarized in Table 4. When more COG is recirculated, the demand for fresh air decreases. This is in line with the earlier findings. However, the situation regarding AOG recirculation is somewhat more intricate. The optimization procedure incorporates a constraint on the steam-to-carbon ratio (S/C greater than 1.5). Further, a lower S/C ratio is favourable for electricity production and system efficiency. The selected solutions in Table 4 belong to different S/C ratios, as these solutions were chosen based on the electrical efficiency and fuel input flow rates. As system electrical efficiency has been analysed in the preceding section, further analysis of electrical efficiency for individual cases will not be pursued.

It is evident that, when aiming to minimize the number of heat exchangers (HEX), warm COG cases inherently feature a higher number of HEX compared to no and hot COG cases. Specifically, in the hot COG case, no additional HEX is needed, given the utilization of a high-temperature blower. To provide a more lucid depiction, it is advisable to direct attention towards the instances of warm COG configuration. Within this subset, the WCCA case stands out with the maximum number of HEX that can introduce complexities in the design and construction of the system. This is primarily attributed to the necessity of cooling AOG flow and partially condensing water. In contrast, the WCWA case comprises sixteen HEX since AOG requires cooling, but no water condensation is involved. However, two steps of water cooling will be combined into one HEX in reality. Remarkably, the WCHA case features the same number of HEX as the WCNA case. As previously stated, the transition from NC to HC does not necessitate additional HEXs, but HC requires a high-temperature blower. In the NCNA case, a substantial HEX area has been observed, which can be attributed to a considerable external water input necessitating evaporation.

To gain a deeper insight into the system heat performance, two possibilities have been explored: the production of high-quality heat at 600 °C and additional electricity generation using a Rankine cycle (RC) [31,32]. As presented in Table 4, when considering identical energy input and electrical efficiency, it becomes evident that NCWA and NCHA cases exhibit optimal thermal performance, capable of supplying 3.45 and 2.94 kW heat, respectively. Indeed, the presented data supports the notion that increased COG recirculation generally results in elevated thermal capacity. However, this outcome is frequently accompanied by a reduction in electrical efficiency. In this study, the selected solutions share similar electrical efficiency. Therefore, it becomes intriguing to understand what factors have the most significant impacts on the thermal efficiency of the system across twelve cases or configurations.

In Figs. 11(a) and (b), the available high-quality heat and external water flow for twelve solutions (one solution for each case) have been presented. The availability of heat at 600 °C is inherently linked to the size and shape of the pocket in the grand composite curve (GCC). However, another crucial factor must be prioritized: external water evaporation. This factor can significantly influence the shape of GCC and can also hinder the availability of high-temperature heat. This is one of the phenomena observed in different cases. As depicted in Fig. 11(a), the WCCA case exhibits the lowest available heat, standing at 0.162 kW. Interestingly, this case also features the highest external water input (Fig. 11b). Further, irrespective of the temperature of high-quality heat, the heat duty remains unchanged, primarily because heat is initially required for water evaporation. In the present analysis, substantial variability is observed in the external water flow across various cases/solutions. This variance is primarily attributable to the constraint imposed on the S/C ratio, which must be maintained above 1.5. Indeed, multi-objective optimization makes it feasible to attain similar electrical efficiency while accommodating different S/C ratios. This flexibility is achieved by carefully considering the effects of other decision variables and objective functions in conjunction with electrical efficiency. However, it is important to note that the heat performance

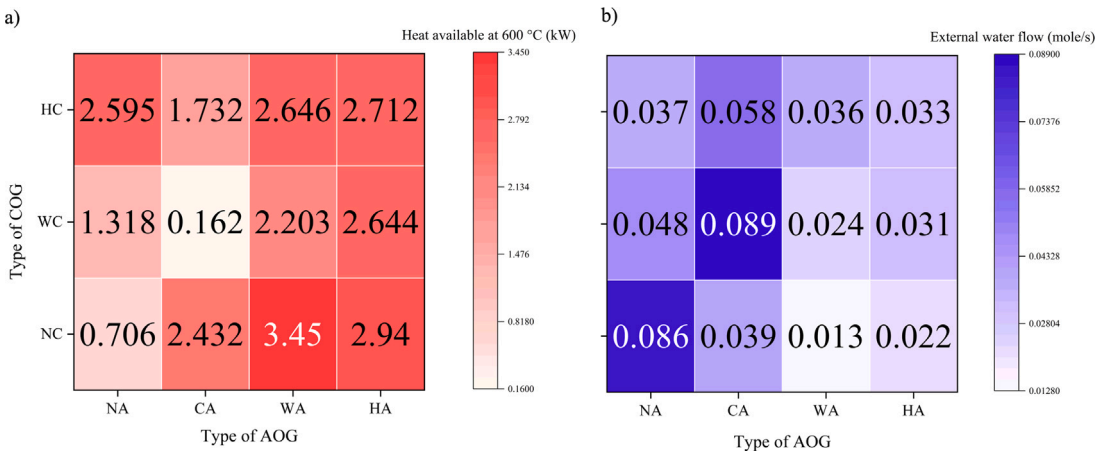

Fig. 11. Performance Comparison for twelve Selected Solutions (One from Each Case): (a) High-quality Heat (kW) Available at 600 °C, (b) External Water Flow (mole/s).

of the system will inevitably differ across all cases. Drawing generic conclusions about heat performance can be challenging, as it hinges on a multitude of interrelated factors and considerations.

A comparative evaluation of NCHA, WCHA, and HCHA cases is necessary to understand the heat performance of no, warm, and hot COG recirculation. Upon comprehensive analysis of various decision variables encompassing fuel input, external water flow, external reforming temperature and ratio, AOG recirculation ratio, and COG recirculation ratio, it is appropriate to compare the performance of NCHA, WCHA, and HCHA cases using the same decision variables. For the comparison, all decision variables have been fixed from the NCHA solution, except the COG recirculation ratio, which has been fixed from the WCHA solution. The results depicted in Fig. 12 are consistent with the published research studies' findings. The HCHA case demonstrates superior thermal performance compared to the other two cases, although this comes at the cost of reduced electrical efficiency. When evaluating system overall efficiency, it is observed that NCHA and WCHA exhibit comparable performance, with both hovering around 86%, while the HCHA demonstrates a slightly lower system overall efficiency of about 84%. Hence, it may be more appropriate to consider the HCHA case in a combined heat and power (CHP) situation, where the major objective is not the production of electricity but rather the optimization of heat generation.

As mentioned earlier, the Rankine cycle has been included to analyse the heat valorization potential for all cases. The percentage contributions to energy output in terms of net electricity, high-quality heat, and RC electricity have been illustrated in Fig. 13 across twelve solutions, one from each case. In general, the additional electricity

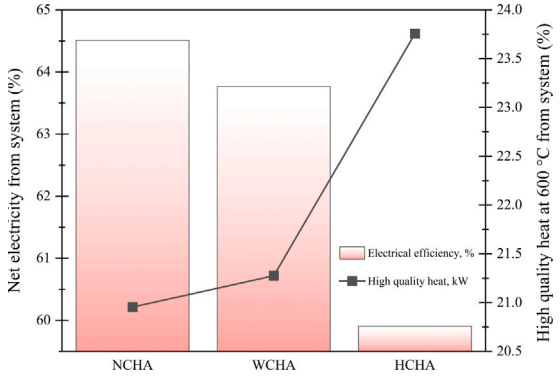

Fig. 12. Impact of COG Recirculation on Electrical Efficiency and Thermal Efficiency (in Hot AOG Case).

generated by the RC tends to be smaller than the availability of high-quality heat, with a few exceptions observed in some cases, namely NCNA, WCNA, and WCCA. In these cases, RC electricity production slightly surpasses high-quality heat generation. This phenomenon could be attributed to the specific shape of the grand composite curve in these cases, indicating that the Rankine cycle can also harvest relatively lower-temperature heat (*e.g.*, heat just above 100 °C). It is noteworthy that, despite the similar electrical efficiency of different solutions or cases, system overall efficiency can vary significantly when incorporating the Rankine cycle, ranging from 66 to nearly 78%.

In this section, a thorough examination was performed on multiple solutions from different cases or configurations with similar values of electrical efficiency and fuel energy input. The main objective of this analysis was to look at the availability and valorization of high-quality heat from the SOFC system. Importantly, the findings of this study show that AOG recirculation primarily affects the use of external water and fuel. Conversely, COG recirculation primarily improves the heat performance of SOFC systems, which unquestionably necessitates a specific set of preconditions. This study reveals that heat performance is highly sensitive to changes in operating conditions. It became evident that the use of hot and warm COG yielded superior heat performance compared to the case without COG recirculation, albeit at the cost of electrical efficiency. Moreover, Rankine cycle integration provided fresh insights, highlighting that system overall efficiency displayed substantial variation even when electrical efficiency remained similar for different solutions or cases. Nevertheless, while heat production is important, the primary objective of SOFC systems is to generate electricity. Therefore, any trade-off between electrical and thermal performance must be carefully considered when deciding on the use of COG.

5. Conclusions

This study conducted a comprehensive analysis to acquire an in-depth understanding of the impacts of anode-off gas and cathode-off gas recirculations on the performance of the SOFC system. A total of twelve potential system configurations were thoroughly examined by performing multi-objective optimization with electrical efficiency, external water usage, AOG recirculation ratio, and air heater duty as objective functions. Important decision variables and practical constraints were included in the optimization problem formulation. After optimization, all configurations can achieve similar electrical efficiency in a system by manipulating decision variables. However, certain configurations, namely WCWA, HCCA, HCWA and HCCA, are inherently constrained in their design, resulting in slightly lower maximum system electrical efficiency compared to other configurations. Further, in the case of

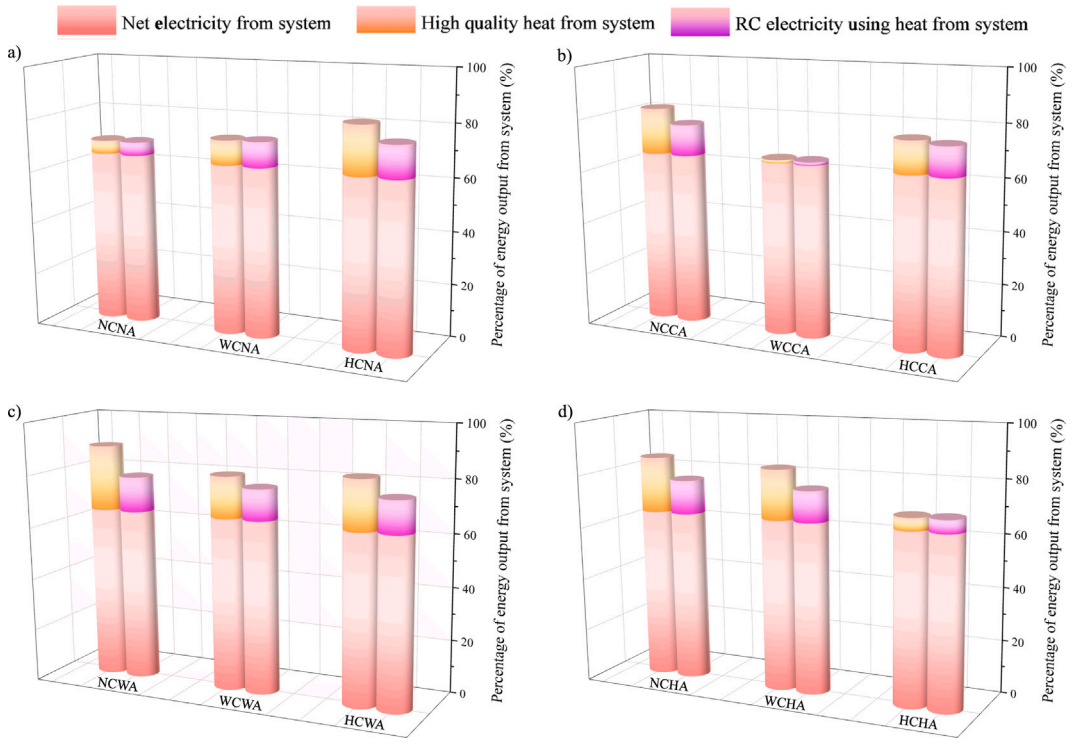

Fig. 13. Energy Output from the System: (a) No AOG (NA) based Cases, (b) Cold AOG (CA) based Cases, (c) Warm AOG (WA) based Cases, and (d), Hot AOG (HA) based Cases.

HCCA, the minimum electrical efficiency of the system can fall below 40%.

An analysis of system performance with different AOG reveals intriguing insights. No, cold and warm AOG cases attain similar system electrical efficiency, but no and cold AOG cases require elevated external water usage, necessitating a larger water purification unit. For the hot AOG cases, the lower efficiency of the AOG blower reduces the system's electrical efficiency, but this case has a direct mixing of heat that can reduce the number of heat exchangers. For COG recirculation, no and warm cases have competitive system electrical efficiency. Further, the warm COG case has a lower fresh air heater duty, affecting heat availability after the stack. For the hot COG case, the system's electrical efficiency is constrained by the lower efficiency of the high-temperature blower. This study also uses a Rankine cycle to evaluate the availability of high-quality heat from the system and its heat valorization potential. The findings revealed that various cases exhibited different thermal performances despite achieving similar system electrical efficiency, making it challenging to derive generic conclusions.

The findings of this study offer valuable insights and recommendations for the integration of SOFC systems across several industrial sectors. In general, the outcomes presented in this study raise two pivotal considerations when determining the suitability of AOG and COG recirculation. Firstly, the size of the SOFC plant must be carefully considered: a demonstration plant or a large-scale plant capable of supplying electricity to a region. This distinction is critical as AOG inclusion can entail additional equipment, such as heat exchangers and recirculation blowers. For small-scale demonstration plants, AOG integration may prove costly and complex. Conversely, AOG integration can yield notable advantages for larger-scale plants, such as enhancing system electrical efficiency, reducing external water consumption, and potentially obviating the need for an external water purification unit. Secondly, the main objective of the designed SOFC systems must be established: power production or combined heat and power production. It is imperative to recognize that, in the context of SOFC systems, electricity production is usually the prime objective. However, in the case of a combined heat and power plant, when both electricity and heat are crucial, including COG recirculation becomes a viable option.

There are several avenues for future research that warrant exploration. Firstly, employing kinetic reactors for the external reformer could establish a link between the external reforming ratio and the operating temperature. Secondly, although this study employed two different methods to analyse waste heat for twelve SOFC system configurations, it would be beneficial to incorporate exergy analysis or designate exergy as one of the objective functions. Thirdly, considering single-pass fuel utilization as a decision variable could yield insightful results. While the optimizer may prioritize high single-pass fuel utilization with minimal AOG recirculation, factors such as external water usage and the required S/C ratio may generate interesting results. Finally, additional objectives such as investment, system size, and others could be included in future research endeavours. These aspects offer promising avenues for expanding our understanding of SOFC systems and enhancing their efficiency and performance.

CRediT authorship contribution statement

Xinyi Wei: Conceptualization, Methodology, Software, Validation, Writing – original draft. **Shivom Sharma:** Conceptualization, Methodology, Software, Validation, Writing – original draft. **Jan Van herle:** Conceptualization, Writing – review & editing, Supervision. **François Maréchal:** Conceptualization, Writing – review & editing, Supervision.

Declaration of competing interest

The authors declare that they have no known competing financial interests or personal relationships that could have appeared to influence the work reported in this paper.

Acknowledgements

The authors thankfully acknowledge the financial support from the project AMON. The project was funded by the European Union under

grant agreement no. 101101521. Views and opinions expressed are, however, those of the author(s) only and do not necessarily reflect those of the European Union or the European Climate, Infrastructure and Environment Executive Agency (CINEA). Neither the European Union nor the granting authority can be held responsible for them. This work was supported by the Swiss State Secretariat for Education, Research, and Innovation (SERI) under contract number 22.00602 - 101101521.

Finally, the authors would like to acknowledge all the editor's and reviewers' constructive feedback to enhance the study's influence.

Data availability

Data will be made available on request.

References

[1] Wei X, Sharma S, Waeber A, Wen D, Sampathkumar SN, Margni M, Maréchal F, Van Herle J. Comparative life cycle analysis of electrolyzer technologies for hydrogen production: Manufacturing and operations. Joule 2024. http://dx.doi.org/10.1016/j.joule.2024.09.007, https://linkinghub.elsevier.com/retrieve/pii/S2542435124004252, S2542435124004252.

[2] Gao P, Zhong L, Han B, He M, Sun Y. Green carbon science: Keeping the pace in practice. Angew Chem, Int Ed 2022;61(46):e202210095. http://dx.doi.org/10.1002/anie.202210095, URL https://onlinelibrary.wiley.com/doi/10.1002/anie.202210095.

[3] Zhang X, Espinoza M, Li T, Andersson M. Parametric study for electrode microstructure influence on SOFC performance. Int J Hydrog Energy 2021;46(75):37440–59. http://dx.doi.org/10.1016/j.ijhydene.2021.09.057, URL https://linkinghub.elsevier.com/retrieve/pii/S0360319921035370.

[4] SolydEra. URL https://solydera.com/en/business-areas-solutions/.

[5] Xu Q, Guo Z, Xia L, He Q, Li Z, Temitope Bello I, et al. A comprehensive review of solid oxide fuel cells operating on various promising alternative fuels. Energy Convers Manage 2022;253:115175. http://dx.doi.org/10.1016/j.enconman.2021.115175, URL https://linkinghub.elsevier.com/retrieve/pii/S0196890421013510.

[6] Facci AL, Cigolotti V, Jannelli E, Ubertini S. Technical and economic assessment of a SOFC-based energy system for combined cooling, heating and power. Appl Energy 2017;192:563–74. http://dx.doi.org/10.1016/j.apenergy.2016.06.105, URL https://linkinghub.elsevier.com/retrieve/pii/S0306261916308807.

[7] Peters R, Deja R, Engelbracht M, Frank M, Nguyen VN, Blum L, et al. Efficiency analysis of a hydrogen-fueled solid oxide fuel cell system with anode off-gas recirculation. J Power Sources 2016;328:105–13. http://dx.doi.org/10.1016/j.jpowsour.2016.08.002, URL https://linkinghub.elsevier.com/retrieve/pii/S0378775316310011.

[8] Jia J, Li Q, Luo M, Wei L, Abudula A. Effects of gas recycle on performance of solid oxide fuel cell power systems. Energy 2011;36(2):1068–75. http://dx.doi.org/10.1016/j.energy.2010.12.001, URL https://linkinghub.elsevier.com/retrieve/pii/S0360544210006912.

[9] Choi E-J, Yu S, Lee S-M. Optimization of operating conditions of a solid oxide fuel cell system with anode off-gas recirculation using the model-based sensitivity analysis. Energies 2022;15(2):644. http://dx.doi.org/10.3390/en15020644, URL https://www.mdpi.com/1996-1073/15/2/644.

[10] Powell M, Meinhardt K, Sprenkle V, Chick L, McVay G. Demonstration of a highly efficient solid oxide fuel cell power system using adiabatic steam reforming and anode gas recirculation. J Power Sources 2012;205:377–84. http://dx.doi.org/10.1016/j.jpowsour.2012.01.098, URL https://linkinghub.elsevier.com/retrieve/pii/S0378775312001991.

[11] Peters R, Deja R, Blum L, Pennanen J, Kiviaho J, Hakala T. Analysis of solid oxide fuel cell system concepts with anode recycling. Int J Hydrog Energy 2013;38(16):6809–20. http://dx.doi.org/10.1016/j.ijhydene.2013.03.110, URL https://linkinghub.elsevier.com/retrieve/pii/S0360319913007507.

[12] Engelbracht M, Peters R, Blum L, Stolten D. Comparison of a fuel-driven and steam-driven ejector in solid oxide fuel cell systems with anode off-gas recirculation: Part-load behavior. J Power Sources 2015;277:251–60. http://dx.doi.org/10.1016/j.jpowsour.2014.12.009, URL https://linkinghub.elsevier.com/retrieve/pii/S0378775314020266.

[13] Zhu Y, Cai W, Li Y, Wen C. Anode gas recirculation behavior of a fuel ejector in hybrid solid oxide fuel cell systems: Performance evaluation in three operational modes. J Power Sources 2008;185(2):1122–30. http://dx.doi.org/10.1016/j.jpowsour.2008.07.027, URL https://linkinghub.elsevier.com/retrieve/pii/S0378775308014742.

[14] Huang Y, Jiang P, Zhu Y. Quasi-two-dimensional ejector model for anode gas recirculation fuel cell systems. Energy Convers Manage 2022;262:115674. http://dx.doi.org/10.1016/j.enconman.2022.115674, URL https://linkinghub.elsevier.com/retrieve/pii/S0196890422004708.

[15] Vincenzo L, Mads Pagh N, Søren Knudsen K. Ejector design and performance evaluation for recirculation of anode gas in a micro combined heat and power systems based on solid oxide fuel cell. Appl Therm Eng 2013;54(1):26–34. http://dx.doi.org/10.1016/j.applthermaleng.2013.01.021, URL https://linkinghub.elsevier.com/retrieve/pii/S1359431113000616.

[16] Engelbracht M, Peters R, Blum L, Stolten D. Analysis of a solid oxide fuel cell system with low temperature anode off-gas recirculation. J Electrochem Soc 2015;162(9):F982–7. http://dx.doi.org/10.1149/2.0371509jes, URL https://iopscience.iop.org/article/10.1149/2.0371509jes.

[17] Liso V, Nielsen MP, Kær SK. Influence of anodic gas recirculation on solid oxide fuel cells in a micro combined heat and power system. Sustain Energy Technol Assess 2014;8:99–108. http://dx.doi.org/10.1016/j.seta.2014.08.002, URL https://linkinghub.elsevier.com/retrieve/pii/S2213138814000721.

[18] Torii R, Tachikawa Y, Sasaki K, Ito K. Anode gas recirculation for improving the performance and cost of a 5-kW solid oxide fuel cell system. J Power Sources 2016;325:229–37. http://dx.doi.org/10.1016/j.jpowsour.2016.06.045, URL https://linkinghub.elsevier.com/retrieve/pii/S0378775316307479.

[19] Peters R, Blum L, Deja R, Hoven I, Tiedemann W, Küpper S, et al. Operation experience with a 20 kW SOFC system. Fuel Cells 2014;14(3):489–99. http://dx.doi.org/10.1002/fuce.201300184, URL https://onlinelibrary.wiley.com/doi/10.1002/fuce.201300184.

[20] Choi E-J, Yu S, Kim J-M, Lee S-M. Model-based system performance analysis of a solid oxide fuel cell system with anode off-gas recirculation. Energies 2021;14(12):3607. http://dx.doi.org/10.3390/en14123607, URL https://www.mdpi.com/1996-1073/14/12/3607.

[21] Wang X, Lv X, Weng Y. Performance analysis of a biogas-fueled SOFC/GT hybrid system integrated with anode-combustor exhaust gas recirculation loops. Energy 2020;197:117213. http://dx.doi.org/10.1016/j.energy.2020.117213, URL https://linkinghub.elsevier.com/retrieve/pii/S0360544220303200.

[22] Wei X, Sharma S, Marechal F, Van Herle J. Design and optimization of a shared heat exchanger network for an integrated rSOC system. In: Computer aided chemical engineering. vol. 52, Elsevier; 2023, p. 1065–70. http://dx.doi.org/10.1016/B978-0-443-15274-0.50170-0, URL https://linkinghub.elsevier.com/retrieve/pii/B9780443152740501700.

[23] Laosiripojana N, Wiyaratn W, Kiatkittipong W, Arpornwichanop A, Soottitantawat A, Assabumrungrat S. Reviews on solid oxide fuel cell technology. Eng J 2009;13(1):65–84. http://dx.doi.org/10.4186/ej.2009.13.1.65, URL http://www.engj.org/index.php/ej/article/view/25/3.

[24] Azami V, Yari M. Comparison between conventional design and cathode gas recirculation design of a direct-syngas solid oxide fuel cell–gas turbine hybrid systems part I: Design performance. Int J Renew Energy Dev 2017;6(2):127. http://dx.doi.org/10.14710/ijred.6.2.127-136, URL http://ejournal.undip.ac.id/index.php/ijred/article/view/14618.

[25] Santin M, Traverso A, Magistri L. Liquid fuel utilization in SOFC hybrid systems. Appl Energy 2009;86(10):2204–12. http://dx.doi.org/10.1016/j.apenergy.2008.12.023, URL https://linkinghub.elsevier.com/retrieve/pii/S0306261908003437.

[26] Saebea D, Patcharavorachot Y, Assabumrungrat S, Arpornwichanop A. Analysis of a pressurized solid oxide fuel cell–gas turbine hybrid power system with cathode gas recirculation. Int J Hydrog Energy 2013;38(11):4748–59. http://dx.doi.org/10.1016/j.ijhydene.2013.01.146, URL https://linkinghub.elsevier.com/retrieve/pii/S0360319913002553.

[27] Chan CY, Rosner F, Samuelsen S. Techno-economic analysis of solid oxide fuel cell-gas turbine hybrid systems for stationary power applications using renewable hydrogen. Energies 2023;16(13):4955. http://dx.doi.org/10.3390/en16134955, URL https://www.mdpi.com/1996-1073/16/13/4955.

[28] Chen J, Chen Y, Zhang H, Weng S. Effect of different operating strategies for a SOFC-GT hybrid system equipped with anode and cathode ejectors. Energy 2018;163:1–14. http://dx.doi.org/10.1016/j.energy.2018.08.032, URL https://linkinghub.elsevier.com/retrieve/pii/S0360544218315524.

[29] Van Veldhuizen B, Van Biert L, Amladi A, Woudstra T, Visser K, Aravind P. The effects of fuel type and cathode off-gas recirculation on combined heat and power generation of marine SOFC systems. Energy Convers Manage 2023;276:116498. http://dx.doi.org/10.1016/j.enconman.2022.116498, URL https://linkinghub.elsevier.com/retrieve/pii/S0196890422012766.

[30] Wencong L, Siyuan L, Zhe Z, Shuzhan B, Guoxiang L, Kongrong M, et al. Performance analysis of a natural gas-fueled 1 kW solid oxide fuel cell-combined heat and power system with off-gas recirculation of anode and cathode. Fuel Cells 2023;23(1):106–18. http://dx.doi.org/10.1002/fuce.202200099, URL https://onlinelibrary.wiley.com/doi/10.1002/fuce.202200099.

[31] Maréchal F, Kalitventzeff B. Process integration: Selection of the optimal utility system. Comput Chem Eng 1998;22:S149–56. http://dx.doi.org/10.1016/S0098-1354(98)00049-0, URL https://linkinghub.elsevier.com/retrieve/pii/S0098135498000490.

[32] Kermani M, Wallerand AS, Kantor ID, Maréchal F. Generic superstructure synthesis of organic Rankine cycles for waste heat recovery in industrial processes. Appl Energy 2018;212:1203–25. http://dx.doi.org/10.1016/j.apenergy.2017.12.094, URL https://linkinghub.elsevier.com/retrieve/pii/S0306261917318172.

[33] Wang L, Zhang Y, Li C, Pérez-Fortes M, Lin T-E, Maréchal F, et al. Triple-mode grid-balancing plants via biomass gasification and reversible solid-oxide cell stack: Concept and thermodynamic performance. Appl Energy 2020;280:115987. http://dx.doi.org/10.1016/j.apenergy.2020.115987, URL https://linkinghub.elsevier.com/retrieve/pii/S0306261920314343.

[34] project E. Nautilus. URL https://nautilus-project.eu.

[35] Simpson A, Lutz A. Exergy analysis of hydrogen production via steam methane reforming. Int J Hydrog Energy 2007;32(18):4811–20. http://dx.doi.org/10.1016/j.ijhydene.2007.08.025, URL https://linkinghub.elsevier.com/retrieve/pii/S036031990700482X.